EXPERIMENTS CONCERNING THE LOW-ENERGY STATES OF N^{16} AND O^{19}

Thesis by

William Zimmermann, Jr.

In Partial Fulfillment of the Requirements

For the Degree of

Doctor of Philosophy

California Institute of Technology

Pasadena, California

1958

ACKNOWLEDGMENTS

It is a pleasure for the author to acknowledge the kind assistance offered him by all of the personnel of the Kellogg Radiation Laboratory. In particular he would like to thank Professors C. A. Barnes, T. Lauritsen, and W. Whaling for their suggestions and advice.

The author is indebted to Dr. F. B. Hagedorn for preparing the N^{15} targets, to Dr. A. O. C. Nier of the University of Minnesota who kindly supplied the O^{18}-enriched gas, and to Dr. R. C. Hanna of the A. E. R. E., Harwell, for his suggestions concerning the measurement of the lifetime of the 0.119-Mev state of N^{16}.

Finally, the author would like to express his appreciation for the financial support given him by the Dow Chemical Company and by the Eastman Kodak Company and for the support given the research by the joint program of The Office of Naval Research and the U. S. Atomic Energy Commission.

ABSTRACT

Angular distributions for four groups of protons from the $N^{15}(d,p)N^{16}$ reaction have been measured using 2.75-Mev deuterons. These groups are those which leave N^{16} in its states at 0, 0.119, 0.293, and 0.392 Mev. The distributions show pronounced stripping characteristics and have been compared to the distributions given by the simple Butler theory. The comparisons indicate that the ground state is formed by the addition of an $l = 2$ neutron to N^{15}, the 0.119-Mev state by an $l = 0$ neutron, the 0.293-Mev state by an $l = 2$ neutron, and the 0.392-Mev state by an $l = 0$ neutron.

The mean life of the 0.119-Mev state has been measured by a beam-chopping technique and is found to be $7.83\ (1 \pm 0.04)$ microseconds.

Angular distributions for three groups of protons from the $O^{18}(d,p)O^{19}$ reaction have been measured, those leaving O^{19} in its states at 0, 0.096, and 1.47 Mev. The distributions of protons leaving O^{19} in its ground state and in its 1.47-Mev state are characteristic of stripping and indicate the formation of the ground state by an $l = 2$ neutron and of the 1.47-Mev state by an $l = 0$ neutron. However, the distribution of protons leaving O^{19} in its 0.096-Mev state does not lend itself to a stripping interpretation.

It is found that the γ-decay of the 1.47-Mev state of O^{19} proceeds mostly to the 0.096-Mev state. The mean life of the 0.096-Mev state has been measured by a recoil technique and

is found to be $1.75(1 \pm 0.16)10^{-9}$ seconds. These observations appear to restrict the possible assignments of spin and parity for the 0.096-Mev state to $J^{\pi} = 3/2^{\pm}$ or $5/2^{+}$.

TABLE OF CONTENTS

I INTRODUCTION

The recent calculations of the properties of certain of the low-energy states in mass 16, 18, and 19 nuclei have given a particular interest to experimental investigations of these states. The calculations which are referred to here are those which have been made on the basis of an intermediate-coupling shell model by Elliott and Flowers (1,2) and by Redlich (3). The following is a description of several experiments undertaken to measure some of the properties of the four low-energy states of N^{16} which occur at 0, 0.119-Mev, 0.293-Mev, and 0.392-Mev excitation and of the three low-energy states of O^{19} which occur at 0, 0.096-Mev, and 1.47-Mev excitation (4).

II THE LOW-ENERGY STATES OF N^{16}

At the outset of this work the ground state of N^{16} had been assigned a spin and parity, J^{π}, of 2^{-} on a basis of the β-decay branching to states of known spin and parity in O^{16} (4,5). However, little was known about the properties of the three other low-energy levels lying within 0.400 Mev of the ground state.

A. Angular Distributions of Protons from the $N^{15}(d,p)N^{16}$ Reaction (6)

Butler and others have pointed out that if certain approximations are valid a (d,p) reaction will proceed by

stripping (7,8). If this is the case, a measurement of the proton angular distribution will enable one to determine the parity of the final state relative to that of the initial state and to restrict the spin of the final state to a few possible values if the spin of the initial state is known. Because the ground state of N^{15} was believed to have the assignment $J^{\pi} = 1/2^{-}$ (Reference 4), the $N^{15}(d,p)N^{16}$ reaction promised to be a useful source of information about the spins and parities of the N^{16} states.

The relative angular distributions of protons leaving N^{16} in its ground and three low-energy excited states were measured using 2.75-Mev deuterons. These bombarding particles were accelerated by the Kellogg Radiation Laboratory 3-Mev Van de Graaff generator and selected in energy by an electrostatic analyzer.

For the relative angular distributions the target was a thin layer of N^{15} atoms embedded in the surface of a nickel foil 1000 Å thick. The target had been prepared with an electromagnetic isotope separator. This separator used nitrogen enriched to 65 percent N^{15} in its radio-frequency ion source and accelerated mass 30 ions to about 20 kev. The thinness of the nitrogen layer meant that the proton groups were well separated from one another in momentum, and the thinness of the nickel backing made observations at forward angles convenient, since the protons could pass through the foil with little momentum loss.

The outgoing protons were resolved in momentum by means of an 180° double-focusing magnetic spectrometer with an acceptance solid angle of 0.00624 steradians. The spectrometer was arranged to transmit protons within a momentum interval equal in size to about 0.9 percent of the total proton momentum. This interval was conveniently larger than the momentum spread within any one group but smaller than the momentum interval between any two groups. A representative momentum spectrum recorded at a laboratory angle of 90° is shown in Fig. 1. The abscissa, fluxmeter current, is inversely proportional to the proton momentum.

The protons which were transmitted by the spectrometer were made to pass through an aluminum foil 0.001 inches thick in front of the detector. This aluminum served to exclude from the detector any deuterons which were transmitted by the spectrometer along with the protons. The detector was a thallium-activated cesium iodide scintillation crystal roughly 0.003 inches thick.

A brief preliminary study of the yields at a laboratory angle of 90° for ten equally spaced deuteron energies from 2.70 Mev to 2.80 Mev showed that the yields were constant with a standard deviation of about $\pm$ 6 percent. This deviation is approximately equal to the statistical uncertainty in each yield that is estimated below. This information was useful as an indication that the regulation of the deuteron energy was not critical.

The principal difficulty with the angular distribution

measurement concerns the proton group leaving N^{16} in its ground state. It was found that protons leaving the 8.32-Mev state of N^{15}, contributed by the $N^{14}(d,p)N^{15}$ reaction, were adding a major amount to the yield in the forward direction. Unfortunately, the two groups were not resolved from each other.

An attempt to evaluate this contribution from the small amount of N^{14} in the target was made in the following way. A target containing natural nitrogen was used to measure the angular distribution of the unwanted group by itself. Then the relative N^{14} content of the two targets was measured by comparing the intensity of the protons leaving N^{15} in its 7.31-Mev state at laboratory angles of 15° and 20°; this group appeared to be isolated from other groups for each target.

The experimental $N^{15}(d,p)N^{16}$ yields, converted to center of mass coordinates, are tabulated in Table I and are plotted as open circles in Figs. 2, 3, 4, and 5. The solid circles in Fig. 2 show in addition the distribution that was obtained before the contaminant group was subtracted. The open circles in Fig. 2, in particular the open circle at about 10° whose ordinate is less than zero, seem to indicate that the amount subtracted was too large. The reason for this is not understood. However, even if the amount subtracted is too large by as much as a factor of two, one may still conclude that the distribution leaving N^{16} in its ground state really has only one forward maximum and that the magnitude

and position of this maximum and the shape of the curve at large angles are not much affected by the contaminant group.

Representative standard deviations for the yields are shown for a number of the points in Table I and in Figs. 2, 3, 4, and 5. These have been computed taking account of several sources of error. First, there is the uncertainty due to counting statistics. Second, there were fluctuations in the yields because the beam spot had the opportunity to fall from run to run on slightly different parts of the target. The target had a somewhat nonuniform surface density of N^{15} atoms. The error due to this effect was estimated from the reproducibility of yields at several angles to be about $\pm$ 5.5 percent. Third, there is an uncertainty due to the slow loss of N^{15} atoms from the target. This loss occurred with beam current surface densities of the order of 0.1 microamperes per square millimeter and is estimated to have amounted to about 12 $\pm$ 6 percent by the end of the runs. The yields were corrected for this loss assuming that it took place uniformly with bombardment, and the uncertainty in the correction was included in the calculated standard deviation.

Another correction to the yields arose from the necessity of changing the orientation of the target in going from laboratory angles greater than 90° to angles less than 90°. Although in each case the target normal made an angle of 45° with the beam, it was found that the yields at 90° differed by 10 percent for the two orientations. This might have been

due to the beam striking slightly different regions of the target or to the presence of wrinkles in the target which may have caused the same portion of the target surface to present different surface densities of N^{15} to the beam in the two cases. It is believed, however, that the error in this correction is small compared to the other errors considered above.

The angles are estimated to be accurate to about $\pm$ 0.4°.

Total relative yields were obtained for each of the proton groups by integrating the angular relative yields over the sphere. These values are presented in Table II. The normalization of these yields is such that if the angular relative yields represent the number of protons per steradian the total relative yields represent the number of protons per sphere.

Table II: Total Relative Proton Yields for the $N^{15}(d,p)N^{16}$ Reaction at a Deuteron Energy of 2.75 Mev

Final State of N^{16}	Total Relative Yield
0 Mev	8410 (1 $\pm$ 0.05)
0.119 Mev	5630 (1 $\pm$ 0.02)
0.293 Mev	9600 (1 $\pm$ 0.03)
0.392 Mev	19700 (1 $\pm$ 0.03)

The standard deviations listed in Table II were computed taking into account the lack of knowledge about the angular relative yields at the far forward and far backward angles where measurements were not made and the uncertainties in the measured points which have already been discussed.

Absolute Cross Sections

A measurement of the absolute differential cross sections for the $N^{15}(d,p)N^{16}$ reactions was made with the spectrometer at a laboratory angle of 90°. The deuteron energy was the same as that used for the angular distributions. This measurement was made by the thick-target technique, which compares the nuclear cross section to a known atomic stopping cross section.

With a thick target the momenta of the outgoing protons run continuously from some maximum value, corresponding to the occurrence of the reaction in the surface of the target, through lower values, which correspond to the occurrence of the reaction at various depths within the target. The target actually need be only thick enough so that the range of outgoing proton momenta is greater than the range transmitted by the spectrometer at any one time. In the present case it was important that the target layer be thin enough to permit the $N^{15}(d,p)N^{16}$ proton groups to be separated from one another. To allow such a thin target the spectrometer was arranged to transmit a narrow range of proton momenta equal in magnitude to about 0.11 percent of the total proton momentum.

The thick-target technique requires a target of known composition. In the present experiment the target consisted of a layer of KNO_3 in which the nitrogen was enriched to 61 percent N^{15}. This layer had been evaporated onto a backing of polished chromium-plated brass. The target was cooled to the temperature of liquid nitrogen in order to inhibit evaporation or dissociation of the KNO_3 under bombardment.

The formula which was used to determine the cross section is the following:

$$\frac{d\sigma}{d\Omega} = \frac{Nz}{E_2}\left(\frac{\cos\theta_1}{\cos\theta_2}\epsilon_2 + \frac{\partial E_2}{\partial E_1}\epsilon_1\right)\frac{eR_p}{2CV\Omega}$$

The meaning of the symbols is as follows:

$\frac{d\sigma}{d\Omega}$ is the differential cross section.

N is the number of protons transmitted by the spectrometer.

z is the amount of charge collected from the beam per incident deuteron, in units of the proton charge. In the present case z = 1 since it was determined experimentally that the H_2^+ content of the incident beam was negligible.

E_2 is the energy of the outgoing protons.

θ_1 is the angle of incidence of the deuterons relative to the target normal. In the present case $\theta_1 = 50°$.

θ_2 is the angle of emission of the protons relative

to the target normal. In the present case $\theta_2 = 40°$.

ϵ_1 is the stopping cross section of the target substance per N^{15} atom for the incident deuterons.

ϵ_2 is the stopping cross section of the target substance per N^{15} atom for the emitted protons.

$\frac{\partial E_2}{\partial E_1}$ is the rate of change of the energy of the outgoing protons relative to that of the incoming deuterons at a given observation angle. This rate is computed from the nuclear dynamics of the reaction.

e is the charge of the proton.

R_p is the spectrometer momentum resolution, defined as the mean momentum of the protons transmitted by the spectrometer divided by the range of momentum transmitted at any one time.

C is the capacitance of the capacitor on which the beam charge is collected.

V is the voltage change of that capacitor during the time that N protons are counted.

Ω is the acceptance solid angle of the spectrometer.

The molecular stopping cross section, ϵ, for KNO_3 was computed from the relationship:

$$\epsilon_{KNO_3} = (1.04)\epsilon_A + \epsilon_N + 3\epsilon_O$$

where $(1.04)\epsilon_A$ is used to approximate ϵ_K. The stopping cross

sections for argon, nitrogen, and oxygen were taken from the compilation made by Whaling (9). The only justification for the approximation for ϵ_K is that at 0.600 Mev the stopping cross section for calcium, whose atomic number is one greater than that of potassium, is 1.08 times the stopping cross section for argon, whose atomic number is one less than that of potassium (9).

The constant of the apparatus, $e\ R_p/2CV\Omega$, was determined by measuring on several occasions the yield of protons scattered elastically by a layer of copper evaporated onto glass. Here again the thick-target technique was applied. It was assumed that the differential cross section was Rutherford below 3 Mev at laboratory angles of 90° and 135°. For the equipment in use in February 1958 with the full spectrometer solid angle, with the 1/16 inch spectrometer resolution slit, and with the 0.1 microfarad "Fast" capacitor of the current integrator #218, the constant was determined to be $(0.222)\ 10^{-8}$ per steradian.

The result of this cross section measurement is most easily given as a number which, when divided into the angular relative yields, gives the differential cross section in millibarns per steradian and which, when divided into the total relative yields, gives the total cross section in millibarns. This number was determined to be 115.

The standard deviation of this number was estimated by combining the statistical errors in the various numbers that were required in the cross section formula. The counting

statistical error in the value of N was estimated to be $\pm$ 4 percent. The stopping powers, ϵ , were assumed to be known to $\pm$ 8 percent. The value of the apparatus constant was thought to be known to $\pm$ 3 percent, which represents the fluctuations from the mean of the several measurements of this quantity. These uncertainties combine to give a standard deviation of $\pm$ 10 percent. However, there is one further consideration. If the KNO_3 had dissociated to KNO_2 in the preparation of the target or during bombardment then the divisor 115 should be increased by about 20 percent.

Comparison of the Experimental Results with Theory

The smooth curves which appear in Figs. 2, 3, 4, and 5 are those given by the simple Butler theory for stripping reactions (Reference 7, Formula 3-26). The determination of these curves was greatly facilitated by the calculations of Lubitz (10). Table III shows the values of the various parameters used in drawing the curves and the values of spin and parity, J^{π} , that are allowed for the final N^{16} states. In this table, l_n is the orbital angular momentum of the captured neutron, r_o expresses in the theory the distance between the target nucleus and the incoming neutron at which they begin to interact, and θ^2 is the neutron reduced width of the final state relative to the single particle limit, $3\hbar^2/2m_c^* r_o^2$, where m^*_c is the reduced mass of the neutron-target nucleus system. The magnitudes of the relative reduced widths are linearly related to the differential cross sections. Thus the reduced widths are really not defined for

the smooth curves until the ordinate scale has been converted to differential cross section units by dividing by 115.

Table III: Stripping Parameters for the $N^{15}(d,p)N^{16}$ Reaction.

Final State in N^{16}	l_n	J^π	Present Results		Warburton and McGruer	
			r_o 10^{-13}cm	$(2J+1)\theta^2$	r_o 10^{-13}cm	$(2J+1)\theta^2$
0 Mev	2	$1^-,2^-,3^-$	(5.7)	0.098	(5.5)	0.27
0.119 Mev	0	$0^-,1^-$	(6.7)	0.020	(4.2)	0.19
0.293 Mev	2	$1^-,2^-,3^-$	(5.7)	0.148	(5.0)	0.33
0.392 Mev	0	$0^-,1^-$	(6.2)	0.092	(4.2)	0.54

Warburton and McGruer have studied this same reaction using 14.8-Mev deuterons (11). The values of l_n that they obtain are in agreement with the present work. However, the values that they obtain for the other parameters in the Butler formula, also shown in Table III, are in rather poor agreement with the present ones. This lack of agreement may simply indicate how inapplicable the Butler theory is for deuteron energies as low as 2.75 Mev. The values of r_o determined here are appreciably larger than the nuclear radius values that are determined by other means. The smallness of the present reduced width values in comparison with those of Warburton and McGruer may possibly be understood as a Coulomb barrier effect, in view of the fact that simple

stripping theory neglects the effect of the Coulomb potential. It is a little surprising, however, that even in the relations between the parameters for the different N^{16} levels there seems to be little correspondence between the two sets of measurements.

As a result of these stripping experiments, of the β-decay studies mentioned previously, and of observations of the deëxcitation of the excited states of N^{16} by γ-radiation (12,13), it has been possible to make plausible the spin and parity assignments for the low energy states of N^{16} which are shown in Fig. 6. Also shown in the figure are the γ-ray branching ratios which have been reported by Freeman and Hanna (13). These are in good agreement with those reported by Wilkinson (12).

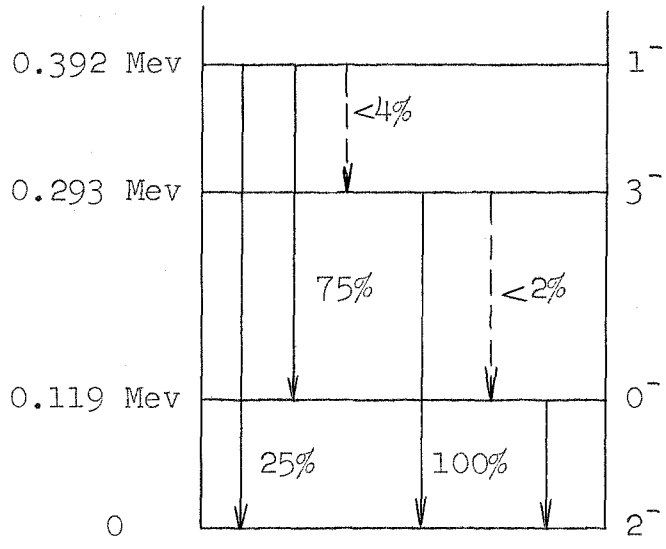

Fig. 6: The Low Energy States of N^{16}

These results compare very favorably with those of the theoretical work of Elliott and Flowers (1). Their work predicts four low-lying odd-parity states for N^{16} having predominantly $p_{1/2}^{-1}\ s_{1/2}$ or $p_{1/2}^{-1}\ d_{5/2}$ configurations. That stripping plays an important role in the formation of each state is indeed consistent with a single particle description of the states.

B. The Lifetime of the 0.119-Mev State of N^{16}

Wilkinson first noted that γ-radiation from the 0.119-Mev state showed a lifetime of the order of several microseconds, supporting the assumption that it is an E2 transition (12). Freeman and Hanna have determined the mean life to be 9.7 (1 ± 0.07) microseconds (13). Both of these experiments used delayed coincidence techniques. The measurement that is described below, on the other hand, employed a beam-chopping technique.

The 0.119-Mev state is produced in the $N^{15}(d,p)N^{16}$ reaction by two routes, by direct formation and by formation of the 0.392-Mev state which then decays to the 0.119-Mev state with a probability of about 75 percent. Since this latter decay is thought to be an M1 transition, its lifetime is expected to be much shorter than several microseconds. Hence the formation of the 0.119-Mev state is expected to be prompt relative to its lifetime by whatever route it is formed. One can then in principle measure its lifetime simply by switching off the deuteron beam and determining the decay rate of the 0.119-Mev γ-ray activity of the target.

A beam of 1.76-Mev deuterons from the Kellogg Laboratory 2-Mev Van de Graaff generator was passed between a pair of parallel electrostatic deflection plates roughly 5 cm long and 1 cm apart before being put through the customary electrostatic energy analyzer. The deflection plates were oriented at right angles to the analyzer plates so that they deflected the beam in a plane parallel to the analyzer plates. A

voltage of about 1.8 kv was sufficient to deflect the beam onto a tantalum stop about 1.5 meters beyond the deflection plates, at the exit of the analyzer. When undeflected, the beam could pass on through a regulating and collimating slit system into a target chamber located about 1.2 meters beyond the tantalum stop.

The target containing N^{15} consisted of a nickel foil 2500 Å thick onto which a layer of titanium of about twice this thickness had been evaporated. This layer of titanium was nitrided by heating it in an atmosphere of NH_3, the nitrogen of which had been enriched to 65 percent N^{15}. However, this layer was contaminated with O^{16} and possibly with more N^{14} than was introduced with the enriched NH_3.

The 0.119-Mev radiation was detected at a laboratory angle of 90° in a cylinder of thallium-activated sodium iodide 1/2 inch long and 1 inch in diameter attached to a Dumont 6292 photomultiplier tube. The inner surfaces of the lead shielding which surrounded the scintillation crystal were lined with 0.010-inch tantalum sheet placed next to the lead and two layers of 0.018-inch tin sheet inside the tantalum. The purpose of the lining was to degrade the energy of the fluorescent X-radiation from the lead and thus produce a cleaner γ-ray spectrum on the low-energy side of the 0.119-Mev photopeak. The pulses from the photomultiplier were sorted in a gated 100-channel pulse height analyzer.

A voltage signal approximating a square wave in shape was applied to the deflection plates. This signal allowed

the beam to remain on the target for about 25 microseconds and then deflected it away from the target for about the same length of time. When the beam was off, the 100 channel analyzer was turned on for an interval of about 8 microseconds. This interval began at a time which could be delayed roughly 1 to 16 microseconds relative to the time that the beam was turned off. A plot of the number of 0.119 Mev γ-ray counts recorded per run versus the delay time used in the run gave directly the decay curve of the radiation.

The runs were normalized by collecting the charge of the deuterons which struck the target. In principle the important quantity for normalization purposes, the sum of the target activities at the beginning of each beam-off period, is not strictly proportional to this charge but is sensitive as well to the shape of the beam current pulse. In order to allow for possible variations in this shape from run to run, an independent monitoring system was provided. This consisted of a gated 10-channel pulse height analyzer which was run from the same photomultiplier. This analyzer was turned on a fixed 2 microseconds after the beam was deflected away from the target and remained on for about 16 microseconds. In practice, the amount of beam charge collected seemed to give just as reliable normalization as the number of monitor counts. Since the amount of charge was simpler to measure, it was used exclusively for most of the runs.

The delay time intervals were measured by using an

oscilloscope to compare the delay signals with the signal from a 4-Megacycle crystal-calibrated frequency standard.

Representative γ-ray spectra showing the region around 0.119 Mev for the extreme delay times are plotted in Fig. 7. The open circles in Fig. 8 represent the average number of counts in the 0.119 Mev photopeak per run as a function of delay time for a representative set of runs. The solid line in Fig. 8 represents the assigned mean life of 7.83 microseconds. This mean life value is the average of the values obtained from several such sets of runs.

The largest source of error in the analysis of this experiment seems to lie in the subtraction of the background from under the photopeak of the 0.119-Mev radiation. It is difficult to determine the shape of this background, and it is not impossible that this shape varies with delay time.

The broken lines in Fig. 8 represent the uncertainty of $\pm$ 4 percent which has been assigned to the value of the mean life. This uncertainty is based on the deviations from the average of the mean life values for the several sets of runs analyzed and on the deviations which were obtained for a range of plausible background subtraction methods applied to any one set of runs.

Several different kinds of runs were made in a search for possible defects in the technique. A target similar in construction to the N^{15} target but containing only natural nitrogen was substituted for the N^{15} target. However, no pulse-height peak or exceptional change in background

appeared in the place of the 0.119-Mev radiation for any of the delay time-settings. The same was true when the beam was allowed to fall on a quartz beam stop, which greatly increased the radiation received by the counter during the time that the beam was on. Several sets of runs were made exposing the scintillation crystal to a constant source of 0.088-Mev γ-rays as well as to the radiation from the N^{15} or the natural nitrogen target. The 0.088-Mev γ-rays were those which result from the e^- decay of Cd^{109} to an excited state of Ag^{109}. The number of counts due to this source remained constant to an accuracy of about $\pm$ 3 percent over the range of delay times.

It may be noted that the mean life value determined here is not in very good agreement with the value 9.7 (1 $\pm$ 0.07) microseconds measured by Freeman and Hanna. The reason for this discrepancy is not understood. A communication from Dr. Hanna concerning this matter was helpful to the author in stimulating the use of the checks on the experiment which are described above, but the difference between the two measurements has not been resolved.

It is interesting to compare these measured lifetimes with the mean life of 3.8 (1 $\pm$ 0.4) microseconds calculated by Elliott and Flowers for this transition taking collective enhancement into account (1). They find that without collective enhancement the lifetime would be expected to be about

1000 microseconds, so that the inclusion of collective effects is important. These authors seem to be content that their estimate is at least of the right order of magnitude.

III THE LOW-ENERGY STATES OF O^{19}

At the time that this work was undertaken the following information had been published about the low-energy states of O^{19}. A study of the β-decay of O^{19} to F^{19} had led to the assignment of a spin and parity, J^{π}, of $5/2^{+}$ to the O^{19} ground state (4,14). The assignment $J^{\pi} = 3/2^{+}$ was believed to be ruled out because the β-decay of O^{19} to the $J^{\pi} = 1/2^{+}$ ground state of F^{19} appeared to have a log $ft \geq 6.5$ and thus to be a forbidden transition.

The spin and parity of the 1.47-Mev state of O^{19} had been determined by means of the $O^{18}(d,p)O^{19}$ reaction which produces that state (15). This reaction was shown to proceed by stripping for 3.01-Mev incident deuterons, yielding a proton angular distribution that is characteristic of the addition of an $l = 0$ neutron to the target nucleus. Since the ground state of O^{18} has the assignment $J^{\pi} = 0^{+}$, the 1.47-Mev state of O^{19} was thus determined to have the assignment $J^{\pi} = 1/2^{+}$. Little information had been acquired about the O^{19} state at 0.096 Mev.

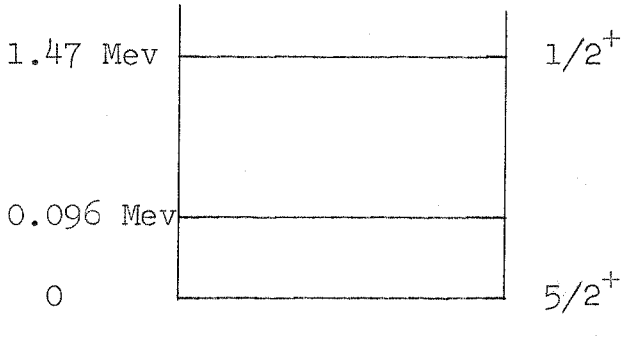

Fig. 9: The Low-Energy States of O^{19}

A. Angular Distributions of Protons from the $O^{18}(d,p)O^{19}$ Reaction.

The principal purpose of this study was to see what role stripping played in the formation of the ground and 0.096-Mev states of O^{19} and to what degree the application of stripping theory would give additional information concerning the spin and parity of these states.

The same equipment that was used to study the $N^{15}(d,p)N^{16}$ proton angular distributions was used for the $O^{18}(d,p)O^{19}$ proton distributions. Thin targets were called for in this experiment likewise, both to resolve the proton groups from the ground and 0.096-Mev states of O^{19} from one another and to resolve these two groups from the group due to the $O^{16}(d,p)O^{17}$ reaction which leaves O^{17} in its ground state (4,15). As in the $N^{15}(d,p)N^{16}$ study, the spectrometer was arranged, for most of the runs, to accept a range of proton momenta larger than the momentum spread within any one of the groups but smaller than the momentum interval between any two groups. A representative momentum spectrum showing the three adjacent groups is shown in Fig. 10 for a deuteron energy of 2.50 Mev and laboratory angle of 90°.

The targets used were thin self-supporting nickel foils having a central region oxidized with O^{18}-enriched oxygen. The foils were either 500 Å or 1000 Å nickel foils which were supplied by the Chromium Corporation of America on copper backings. One procedure for preparing them is described by Bashkin and Goldhaber (16); they are first mounted in stain-

less steel clamping frames and then are immersed in acid to dissolve away the copper backing. An alternative procedure was found which avoided the necessity of acid-resisting target frames and which made washing somewhat simpler.

The piece of foil to be mounted was floated on a small pool of activated chromic acid solution with the copper side down. After the copper had dissolved but before the acid had wet the upper surface of the foil the acid was drawn off with a medicine dropper and replaced with several exchanges of distilled water to wash the foil. Finally, the foil was mounted by being lifted from the surface of the water on a thin flat target frame which was brought up from below, inclined to the water surface. A self-supported circular area 0.7 cm in diameter could be prepared this way. The nickel surfaces tended to be slack after mounting, but this turned out to be of advantage in the oxidation process.

The foils were oxidized by using the technique described by Holmgren et al. (17). This involved heating the foils in an oxygen atmosphere with a focused spot of light from a projection lantern. The pressure of the O^{18}-enriched oxygen gas was typically held at about 5 cm of mercury during the heating. Most of the foils seemed to contract before the temperature reached the oxidation point, and for this reason the more loosely mounted foils were less susceptible to tearing during heating than were the tighter ones.

Relative angular distributions were measured at a

deuteron energy of 1.74 Mev for the proton groups which leave O^{19} in its states at 0 Mev, 0.096 Mev, and 1.47 Mev. Distributions for the groups leaving the first two of these states were also measured at a deuteron energy of 2.50 Mev. The relative yields have been converted to center of mass coordinates and are tabulated in Tables IV and V and plotted in Figs. 11 and 12. In addition, excitation curves for the first two groups were measured at a laboratory angle of 90° for deuteron energies between 1.7 and 2.6 Mev. The yields for these curves are given in Table VI and are shown in Fig. 13.

At the same time that some of the above measurements were made, the proton group from the $O^{16}(d,p)O^{17}$ reaction leaving O^{17} in its ground state was observed for reference purposes. Table VII and Fig. 14 give the angular distribution of this group in center of mass coordinates for a deuteron energy of 2.50 Mev, and Table VIII and Fig. 15 give the excitation curve at a laboratory angle of 90° for deuteron energies between 1.8 and 2.7 Mev. The information in Fig. 15 has been supplemented by some additional information, shown by the solid circles, which was obtained using a scattering chamber and a target prepared from natural oxygen.

The relative yields for the various curves showing the $O^{18}(d,p)O^{19}$ reactions were measured with several different targets but have all been normalized to each other. The same is true for the yields in the two curves showing the

$O^{16}(d,p)O^{17}$ reaction.

Standard deviations for the yields have been listed for a number of points throughout the tables and have been shown in the accompanying figures wherever feasible. Most of these standard deviations refer only to the particular curve in which the point for which they are calculated lies. The additional errors involved in the relative normalization of all of the curves for the $O^{18}(d,p)O^{19}$ reaction are mentioned in the text below.

A major source of error in the relative angular distributions at a deuteron energy of 2.50 Mev and in the excitation curves is thought to have arisen from the slow loss of oxygen from the target during bombardment and the resulting non-uniformity of the oxygen surface density. This loss seemed to occur with beam current intensities of the order of 0.1 microampere per square millimeter.

Errors due to variations of the beam alignment on the nonuniform target surface were estimated by considering the reproducibility of yield measurements repeated at the same angles and energies within short time intervals. It was determined to what extent the variations in these yields exceeded those expected from counting statistics alone. In the case of the angular distributions at 2.50 Mev the standard deviation which described these variations was found to be $\pm$ 2 percent, while for the excitation curves it was $\pm$ 3.5 percent.

In order to allow for the slow loss of the target oxygen

and for major changes in the alignment of the beam, as well as for differences between the two targets used, the various runs which were made for different portions of the 2.50-Mev angular distributions and of the excitation curves were normalized to each other at common energies and angles. In the case of the 2.50-Mev angular distributions the maximum difference in normalization factors for one target was about 7 percent, while for the excitation curves the maximum difference was 16 percent.

The uncertainties in the normalization factors were estimated from the uncertainties in the yields at the comparison points from which the factors were computed. The uncertainties in the yields were those mentioned above due to target nonuniformity combined with those due to counting statistics. The errors in normalization for the angular distributions ranged up to about $\pm$ 7 percent while those for the excitation curves averaged about $\pm$ 5 percent. The indicated standard deviations for the points in the 2.50-Mev angular distributions and in the excitation curves are then a statistical combination of these normalization errors, the errors due to nonuniformity of the target, and errors due to counting statistics.

In the case of the angular distributions at a deuteron energy of 1.74 Mev, it was found that by using sufficiently low beam intensities on a fresh target it was possible to avoid the problems of oxygen loss and nonuniformity. Variations in repeated measurements at the same points were well

accounted for by counting statistics alone. For this reason only counting statistics were used to compute the standard deviations for these angular distributions.

The angular distribution at 1.74 Mev for the proton group leaving the 1.47-Mev state of O^{19} required a special correction. The correction arose because this group had a low enough momentum and a large enough momentum spread so that there no longer existed a small range of spectrometer coil currents at any one observation angle for which the entire group was transmitted by the spectrometer. As a result the number of counts recorded at the peak of the momentum profile no longer represented the full yield of the group.

The correction to be applied to the peak number of counts was estimated at several angles by measuring both the peak number of counts and the full momentum profile of the group. The full yield, Y, was determined from the momentum profile by the expression:

$$Y = R_p \int \frac{N(p_2)\, dp_2}{p_2}$$

The meaning of the symbols is as follows:

R_p is the momentum resolution of the spectrometer, defined in Part II A.

P_2 is the mean momentum of the protons transmitted by the spectrometer at a point in the profile.

$N(p_2)$ is the number of protons transmitted by the spectrometer at that point.

The integral is taken over all the values of p_2 for which N is non-zero.

The correction amounted to about 5 percent at many angles but rose as high as 20 percent for some of the angles greater than 90°. It is believed that this correction contributed a negligible error to the relative angular distribution, but it is estimated that it caused an uncertainty of about $\pm$ 6 percent in the normalization of this angular distribution to the other two distributions measured at the same deuteron energy. This uncertainty stemmed principally from an uncertainty in the value of R_p for the spectrometer.

The angular distributions at 1.74 Mev were normalized to the excitation data and to the distributions at 2.50 Mev with an uncertainty due to counting statistics of about $\pm$ 2 percent.

It is estimated that the angles are known to about $\pm$ 0.4°. The uncertainty in the deuteron energy scale is perhaps $\pm$ 0.5 percent.

Total relative yields were obtained for each of the proton groups by integrating the angular relative yields over the sphere. The results are given in Table IX. The normalization of these total yields is such that they represent yields per sphere if the angular yields are regarded as representing yields per steradian.

Table IX: Total Relative Yields

Reaction	Final State	Deuteron Energy	Total Relative Yield
$O^{18}(d,p)O^{19}$	0 Mev	1.74 Mev	4820 (1 ± 0.03)
		2.50 Mev	6610 (1 ± 0.03)
	0.096 Mev	1.74 Mev	1140 (1 ± 0.05)
		2.50 Mev	1270 (1 ± 0.05)
	1.47 Mev	1.74 Mev	20630 (1 ± 0.07)
$O^{16}(d,p)O^{17}$	0 Mev	2.50 Mev	74700 (1 ± 0.02)

The standard deviations stated in Table IX are a statistical combination of several errors: the error due to uncertainties in the shape of the angular distributions at the far forward and far backward angles, the error resulting from the errors in the individual points discussed above, and, in the case of the $O^{18}(d,p)O^{19}$ reactions, the error associated with the normalization of the various angular distributions.

Absolute Cross Sections

An estimate of the absolute cross section for the $O^{16}(d,p)O^{17}$ reaction may be made by using the absolute measurements of Stratton et al. (15). There are two points in common between that work and the present, a deuteron energy of 2.65 Mev and center of mass angle of 93.8°, for which the center of mass differential cross section is given as 11.3 (1 ± 0.04) millibarns per steradian, and a deuteron energy

of 2.50 Mev and center of mass angle of 53°, for which the differential cross section is 18.0 (1 ± 0.06) millibarns per steradian. The ratio between the yield measured in the present work and the cross section is 403 for the first point and 385 for the second. Thus one may convert the $O^{16}(d,p)O^{17}$ angular relative yields to millibarns per steradian and the total relative yield to millibarns by dividing them by the average ratio, 394.

The $O^{18}(d,p)O^{19}$ cross sections may be estimated very roughly by a guess that the O^{18}/O^{16} ratio in the target was 0.24 (1 ± 0.3). The O^{18}/O^{16} ratio for the oxygen gas from which the targets were made was thought to have been 0.31 when the gas was first obtained. However, there seems to exist the possibility that in the preparation of the targets the gas might have been contaminated with natural oxygen. The O^{18} yields should thus be divided by 95 (1 ± 0.3) in order to obtain an estimate of the absolute cross section.

Comparison of the Experimental Results with Theory

The angular distribution of protons leaving O^{19} in its ground state at a deuteron energy of 2.50 Mev shows the forward maximum typical of a stripping distribution and indicates the capture of an $l = 2$ neutron by O^{18} to form the ground state of O^{19}. The $l = 2$ assignment is based on a comparison of the angular position of the maximum of the experimental distribution with that of the distribution given by the simple Butler theory. It is found that a value of

$r_o = (5.7)10^{-13}$ cm must be used in the theoretical expression for $l = 2$ to make the maxima coincide. Although large compared to nuclear radius values determined in other ways, this value compares well with the values for r_o needed in Part II A for the $N^{15}(d,p)N^{16}$ reaction. The corresponding angular distribution at a deuteron energy of 1.74 Mev shows somewhat less sign of stripping, in agreement with the expectation that the theory becomes less applicable as the deuteron energy decreases.

An $l = 2$ neutron might combine with the $J^\pi = 0^+$ ground state of O^{18} to form either a $3/2^+$ or a $5/2^+$ state of O^{19}. These possibilities for the ground state of O^{19} are quite consistent with the β-decay results. It is a little unfortunate that the stripping results do not help to strengthen the preference of $J^\pi = 5/2^+$ over $J^\pi = 3/2^+$ that is derived from the β-decay work.

The angular distribution of the weak proton group leaving O^{19} in its 0.096-Mev state is almost isotropic for a deuteron energy of 2.50-Mev. The absence of the characteristics of stripping suggests that the neutron reduced width of the state is small.

Ahnlund finds that at a deuteron energy of 0.88 Mev the intensity of the proton group leaving O^{19} in its 0.096-Mev state rises significantly in the forward direction (18). There is, indeed, some sign of this tendency at a deuteron energy of 1.74 Mev. Although Popić analyzes Ahnlund's data as if it were an $l_n = 1$ stripping distribution (19), it is

perhaps not clear that the forward rise can be understood so simply, in view of the tendency of this effect to disappear at higher deuteron energies.

The proton distribution leaving O^{19} in its state at 1.47 Mev appears to show an $l_n = 0$ stripping shape, even though the deuteron energy of 1.74 Mev is quite low for stripping theory to apply well. This l value is in agreement with the value determined by Stratton et al. at a deuteron energy of 3.01 Mev (15).

B. Gamma-Ray Transitions in O^{19}.

A sodium iodide scintillation pulse height spectrum of γ-rays from an 1000-Å O^{18}-enriched NiO target showed 0.096-Mev and 1.37-Mev γ-rays when the target was bombarded with 1.74-Mev deuterons. However, the intensity of any 1.47-Mev γ-rays was less than 0.2 of the intensity of the 1.37-Mev γ-rays. The intensity of the 0.096-Mev γ-rays and the absence of 1.47-Mev γ-rays suggested that the 1.47-Mev state of O^{19} preferred to decay to the 0.096-Mev state rather than to the ground state. This measurement was not very definitive, however, since 1.35-Mev γ-rays are produced following about 70 percent of the beta-decays of the O^{19} ground state and may also be produced in the $O^{18}(d,n)F^{19}$ reaction. These 1.35-Mev γ-rays would, of course, not have been distinguished from the 1.37-Mev γ-rays.

A more conclusive measurement was undertaken to investigate the suggestion made above, again using the $O^{18}(d,p)O^{19}$ reaction. The procedure was to measure the yield of the 0.096-Mev γ-rays in relation to the total yields of protons leaving O^{19} in its 0.096-Mev and 1.47-Mev states.

This experiment was carried out with the same equipment that was used to measure the proton angular distributions. The proton spectrometer was placed at a laboratory angle of 30° and observed the $O^{18}(d,p)O^{19}$ proton group which leaves the O^{19} nucleus in its 1.47-Mev state. At the same time 0.096-Mev γ-rays were detected in a shielded sodium iodide scintillation counter placed at a laboratory angle of 90°,

and the pulses were sorted in an 100 channel pulse height analyzer. The bombarding deuteron energy was 1.74 Mev. Because proton angular distributions had been measured at this energy, it was possible to infer from the number of protons counted the total number of O^{19} nuclei formed in the 0.096-Mev and 1.47-Mev states.

The total 0.096-Mev γ-ray yield was calculated from the number of counts recorded in the γ-ray counter assuming that the emission was isotropic in the laboratory system. In so far as compound nuclear processes are involved in the formation of the 0.096-Mev state, the high excitation energy in F^{20} and the absence of marked resonance behavior in the excitation function make it likely that many states of different angular momenta contribute to this reaction in no simple phase relationship and that no marked angular effects are produced. The 1.47-Mev state, of course, is thought to be $J = 1/2$, and so any radiation which follows its formation must be isotropic.

In analyzing the γ-ray spectra care was taken not to include counts which might have been associated with 0.110-Mev γ-radiation from F^{19}. Such radiation might have been produced by the $O^{18}(d,n)F^{19}$ reaction. Because the photopeak of the 0.096-Mev radiation had a width at half-maximum of about 16 percent, the two γ-rays could not be well resolved from one another. The only evidence for the presence of any 0.110-Mev γ-radiation was a broadening of the low part of the high-energy side of the 0.096-Mev photopeak. The effects

of the 0.110-Mev γ-radiation were avoided by summing up the counts in only the low-energy portion of the 0.096-Mev photopeak. Then the proportion of the total number of 0.096-Mev γ-ray counts that this sum represented was estimated by using the clean spectrum of the 0.088-Mev γ-radiation from a Cd^{109} source.

The ratio of the number of protons leaving O^{19} in its 0.096-Mev state to the number of 0.096-Mev γ-rays was found to be 0.05 (1 ± 0.1), and the corresponding ratio for the 1.47-Mev state was found to be 0.91 (1 ± 0.14). The standard deviations stated here are a combination of a $\pm$ 12 percent uncertainty in the measurement of the γ-ray yield with somewhat smaller errors in the determination of the total proton yields.

The major uncertainty in the measurement of the γ-ray yield arose from the freedom of choice of method of background subtraction and was estimated to be $\pm$ 10 percent. The other uncertainties considered were a $\pm$ 5 percent uncertainty due to fluctuations in the number of γ-ray counts from run to run, a $\pm$ 3 percent uncertainty in the correction for the γ-ray attenuation in the lucite target-chamber window, a $\pm$ 3 percent uncertainty in the estimate of the relation between the number of counts in the low-energy portion of the photopeak and the total number of γ-rays stopped by the crystal, and, finally, a $\pm$ 2 percent uncertainty in the proportion of all of the γ-rays emitted that were stopped by the crystal.

The uncertainties in the total proton yields arose from an uncertainty of about ± 2 percent in the normalization of the present yields to the yields in the angular distribution work of Part III A combined with the uncertainties described in that part concerning the computation of the total relative yields from the angular relative yields. The total uncertainty in the proton yield leaving the 1.47-Mev state of O^{19} was estimated to be about ± 4 percent while that for the 0.096-Mev state was about ± 8 percent.

These measurements make it plausible that the 1.47-Mev state of O^{19} decays almost entirely to the 0.096-Mev state in preference to the ground state. This would suggest that because an E2 transition is allowed to the ground state the transition to the 0.096-Mev state is E1 or M1 with E2 a third, less likely possibility. These alternatives would allow the 0.096-Mev state to have the assignment $J^{\pi} = 1/2^{\pm}$ or $3/2^{\pm}$, with $5/2^{+}$ a less likely possibility. The lifetime experiment described below is believed to rule out the possibilities $J^{\pi} = 1/2^{\pm}$.

C. The Lifetime of the 0.096-Mev State of O^{19}.

When this work was begun there existed the possibility that the 0.096-Mev state of O^{19} might have a lifetime comparable to or longer than that of the 0.119-Mev state of N^{16}. However, a preliminary investigation with the same apparatus used to measure the lifetime of the N^{16} state revealed that the mean life of the 0.096-Mev state was less than about 2 microseconds.

The measurement of the lifetime was carried out using a recoil technique. This involved observing directly the distance that excited O^{19} nuclei, recoiling from the $O^{18}(d,p)O^{19}$ reaction, traveled in vacuo before decaying. A detail of the apparatus is shown in Fig. 16.

A beam of 1.74-Mev deuterons from the Kellogg Laboratory 2-Mev Van de Graaff generator was allowed to pass through a thin, self-supported, O^{18}-enriched NiO target such as was used for the proton angular distributions. A nickel foil thickness of 500 Å was chosen in order that the recoiling O^{19} nuclei would not lose a large portion of their velocity in the target. The beam spot area was typically a square 0.06 inches on a side.

As was brought out in Part III B, most of the 0.096-Mev γ-rays arose from O^{19} nuclei which were first produced in the 1.47-Mev state. All of the O^{19} nuclei so formed recoiled initially in the forward direction within a cone of half-angle 48°. As these excited recoil nuclei decayed to the 0.096-Mev state there was additional momentum imparted to

the nucleus, but this momentum was small compared to the total momentum of the nucleus and has been neglected here. The O^{19} nuclei which were formed in the 0.096-Mev state directly also recoiled in the forward direction but within a cone of half-angle 79^{o}.

The γ-ray counter was provided with a collimator through which could be seen a narrow region of the space just following the target. For reasons of convenience it was the target rather than the collimator and counter that was moved to vary the distance between the target and the region seen by the counter. The target was moved and its position measured by means of a precision screw having a pitch of 40 threads per inch.

The critical edges of the collimator were made of tungsten. These edges were very sharp for the low-energy 0.096-Mev γ-radiation compared to the range of distances from the target being measured. The 0.096-Mev γ-rays were detected in a square prism of thallium-activated sodium iodide 1 inch by 1 inch by 3/8 inch which was shielded from stray radiation by lead lined in the same fashion as it was lined for the N^{16} lifetime experiment. The pulses from the DuMont 6292 photomultiplier were sorted in an 100 channel pulse height analyzer.

One set of runs was made with the tungsten collimator plates separated by a gap of 0.062 inches, as is shown in Fig. 16. Another set was made with a collimator plate spacing of 0.125 inches. The following discussion refers speci-

fically to the first set although the analyses of the two sets were similar. Fig. 17 shows representative γ-ray pulse height spectra for three runs in the first set, each one with a different relative position of the target. These spectra are accompanied by a reference spectrum due to 0.088-Mev γ-rays from a Cd^{109} source which is shown in Fig. 18. This spectrum was taken shortly before the spectra in Fig. 17 with the same pulse amplification.

For each run, a number proportional to the number of 0.096-Mev γ-rays detected was computed by subtracting the background from the sum of the counts in the six highest channels of the 0.096-Mev photopeak. The background for these channels was determined in two ways and the mean of the determinations was used. One way was to draw by eye a background line connecting the minimum in the spectrum at the left of the peak to the flat portion of the spectrum to the right. The other was to assume that the background was well represented by the spectrum in the vicinity of channel number 57.

There was the possibility in this experiment, as there was in the γ-ray yield measurements of Part III B, that 0.110 γ-radiation from F^{19} was present. There is some evidence of this radiation in the spectrum at the bottom of Fig. 17 where the low part of the high-energy side of the peak is less steep than that of the Cd^{109} reference spectrum in Fig. 18. It is believed, however, that a sum over the six highest channels in the 0.096-Mev photopeak was not appreciably influenced by whatever 0.110-Mev radiation was

present.

The relative numbers of 0.096-Mev γ-rays per run are represented by open circles plotted in Fig. 19 as a function of the relative target position. Each point is typically an average of three runs of the type shown in Fig. 17. The normalization of the ordinate scale and the choice of origin for the abscissa scale in Fig. 19 were not determined by the experiment but were chosen so as to give the best fit to the smooth curve which appears in the same figure. This smooth curve is a calculated curve and is discussed below. Only the four lowest points were appreciably affected by the method of background subtraction. The ordinate of the lowest of these points would be about 30 percent larger than it is for the first method alone and about 30 percent smaller for the second.

In view of the fact that most of the 0.096-Mev γ-radiation is preceded by 1.37-Mev radiation from the 1.47-Mev state, the experiment described so far does not distinguish which of the two excited states involved is showing the observed lifetime. An attempt was made to use the same apparatus to verify directly that the 1.37-Mev γ-radiation did not itself show a comparable lifetime.

For this experiment the sodium iodide crystal was turned through 90° in order that the γ-rays might traverse a greater thickness of crystal than before. The crystal was also moved farther away from the collimator so as to aid the collimator in its selectivity. For these runs the

tungsten plates had a separation of 0.062 inches. Additional lead shielding was placed between the collimator and the crystal, partly to improve the collimation and partly to help prevent any of the 1.35-Mev γ-radiation which follows about 70 percent of the O^{19} β-decays from reaching the crystal.

The results were rather inconclusive. This was due in part to the smallness of the number of counts in the full-energy peak of the 1.37-Mev γ-ray spectrum and to the presence of a relatively large background which climbed steeply in the low-energy direction. In addition, the collimator edges were much less sharp for this energy γ-ray than they were for the low-energy one. The rate of decrease of the 1.37-Mev γ-ray intensity as the target was moved appeared to be perhaps somewhat greater than 3 times the rate for the 0.096-Mev γ-ray. It is believed that this rate was not significantly different from the rate that one would have observed for a γ-ray of this energy emitted from a state of vanishing lifetime.

Calculation of the Mean Life

The smooth curve which appears in Fig. 19 is a curve calculated for a mean life of $(1.70)\ 10^{-9}$ seconds. It was assumed for this calculation that all of the O^{19} nuclei formed in the 1.47-Mev state contributed to the 0.096-Mev γ-radiation by decaying to the 0.096-Mev state rather than to the ground state. It was assumed also that the lifetime of the 1.47-Mev state is short compared to the lifetime of

the 0.096-Mev state. A third assumption was that the 0.096-Mev γ-rays were emitted isotropically in the system of the recoiling nucleus. This was thought to be justified by the same considerations that were invoked in Part III B to justify a related assumption.

The first step in making this calculation was to determine the direction and velocity of an excited O^{19} recoil nucleus in terms of the direction of the proton emitted with it. It was then necessary to correct the ion velocity for the loss of velocity suffered in escaping from the target. No attempt was made, however, to correct the direction of motion of the O^{19} recoils for any large-angle scattering in the target. Next, the probability that an excited recoil nucleus with a mean life τ would reach a certain perpendicular distance from the target before decaying was computed as a function of the direction of emission of the coincident proton. Then, a sum over all proton directions was performed using the proton angular yields that had already been measured for the deuteron energy of 1.74 Mev.

An analytical expression for the calculations described above may be given as follows:

$$N\left(\frac{z}{\tau}\right) = N_0 \int_{-1}^{+1} I(\cos\theta)\; e^{-\frac{z}{\tau\, v(\theta_R)\cos\theta_R}}\; d(\cos\theta)$$

The meaning of the symbols is as follows:

z is the perpendicular distance from the target, increasing in the direction of the deuteron beam.

τ is the mean life of the decaying state.

θ is the polar angle describing the direction of emission of the proton measured in the center of mass system.

θ_R is the polar angle describing the direction of emission of the recoil measured in the laboratory system.

$v(\theta_R)$ is the velocity with which a recoil emitted with polar angle θ_R emerges from the target.

$I(\cos\theta)$ is the relative yield of protons per unit solid angle in the center of mass system which are emitted with a polar angle θ .

$N(z/\tau)$ is the number of recoils of mean life τ which attain a perpendicular distance from the target greater than z before they decay.

N_o is just some convenient normalizing factor.

The relationship between θ_R and θ is given by the expression:

$$\cos\theta_R = \frac{k_R - \cos\theta}{\sqrt{1 + k_R^2 - 2k_R\cos\theta}}$$

where k_R is the ratio of the velocity of the center of mass in the laboratory system to the velocity of the recoil in the center of mass system. The function $v(\theta_R)$ is given by the expression:

$$v(\theta_R) = v_{cm} \frac{k_R - \cos\theta}{k_R \cos\theta_R} - \Delta v$$

where v_{cm} is the velocity of the center of mass in the laboratory system and Δv is the amount of velocity that the recoil loses in escaping from the target.

The integral above was evaluated by numerical means for each of the two modes of formation of the 0.096-Mev state, and the results were added together to give a function that may be called $N_s(\frac{v}{\tau})$. The function that describes the number of recoils that decay in view of the counter is given by $N_s(\frac{v}{\tau}) - N_s(\frac{v+\Delta v}{\tau})$, where Δz is the interval of z along the beam axis that is seen by the counter. This last function is the one which was used to construct the smooth curve.

The correction for the recoil's loss of velocity in the target was made by constructing curves representing the recoil's velocity as a function of its range expressed in surface density units. A curve was constructed for O^{19} recoils in the NiO target and for O^{19} recoils in the carbon surface layer which appeared on the target during bombardment. The velocities of the recoils in this experiment lay between 0 and $(2.5)10^8$ cm/sec.

For the construction of the curves an attempt was made to compare the rather sparse information available on the stopping of moving atoms (9, 20, 21, 22, 23). This comparison was based on the assumption that $dv/d\rho$, the rate of change of the atom's velocity per unit surface density of stopping material, may be expressed as a product $f(a)g(s)h(v)$. Here $f(a)$ is a factor which depends on the atom being stopped, $g(s)$ a factor which depends on the stopping material, and $h(v)$ a function of the atom's velocity. The form of $h(v)$ that is suggested by some of the experimental work is $1/v$ for velocities up to about $(1.2)10^8$ cm/sec and constant for the velocities of interest above that velocity, with a smooth transition at $(1.2)10^8$ cm/sec. This form was used for the construction of the curves, and the values which were chosen for $dv/d\rho$ in the constant region are as follows:

O^{19} atoms in NiO: $dv/d\rho = (4.9)10^5$ cm $sec^{-1}/\mu gm$ nickel cm^{-2}

O^{19} atoms in C: $dv/d\rho = (9.3)10^5$ cm $sec^{-1}/\mu gm$ carbon cm^{-2}

A standard deviation of $\pm$ 30 percent was assigned to the velocity scale of the stopping curves. This applies to both the value of velocity at which the transition occurs and to the values of $dv/d\rho$ everywhere along the curve. The standard deviation is quite large because there appeared to be a large disagreement between the value of $dv/d\rho$ determined from some direct measurements for O^{16} atoms in copper (20) and the value determined by an extension to nickel of some

measurements for atoms stopping in air and argon.

The surface density of nickel in the target was determined both from the nominal thickness of the foil, 500 Å, and by elastic proton scattering, the former value lying about 20 percent below the latter. An average value of 49 μgm nickel/cm^2 was adopted. The calculations were made by making the approximation that all of the recoils originated in the middle of the target layer and thus had to pass through a NiO layer corresponding to one half of the nickel density measured above.

The surface density of carbon on both sides of the target combined was determined by the $C^{12}(d,p)C^{13}$ reaction at a bombarding deuteron energy of 2.84 Mev and a laboratory angle of 135° using the cross sections given in the literature (24, 25). The value obtained for the surface density of carbon after the target had been used for a set of recoil runs was about 4 ± 3 μgm/cm^2. Assuming that the carbon layer built up linearly with bombardment during the recoil runs, the average recoil had to pass through a layer of roughly one quarter this thickness, and the correction to its velocity for the carbon layer was very small.

The final value of the mean life, which was determined from the set of runs shown in Fig. 19 and from the set measured with a 0.125 inch collimator spacing, is $1.75(1\pm0.16)10^{-9}$ seconds. The standard deviation is based mainly on two sources of uncertainty. The first source was mentioned earlier and concerns the amount of background to be subtracted

from the γ-ray photopeaks. It is thought that this uncertainty produces an uncertainty in the lifetime of about $\pm$ 10 percent.

The second source is the uncertainty in the rate of stopping of O^{19} atoms in the target. It is estimated that this uncertainty produces an uncertainty in the time scale of the calculated curve of perhaps $\pm$ 12 percent. This is, of course, an over-simplification of the situation since the uncertainty is not only one of time scale but also of shape, due to the fact that the low-velocity recoils are influenced more than the high-velocity ones. It may be seen in Fig. 19 that the calculated curve is not quite of the proper shape to fit the points well. The calculated curve lies above the experimental points for target positions in the region of 0.08 cm. It is found that if lower values of $dv/d\rho$ and a correspondingly lower value of mean life are used the shape agreement becomes worse. On the other hand, if larger values of $dv/d\rho$ and a correspondingly larger value of mean life are used the agreement is improved. This would suggest that the values of $dv/d\rho$ adopted were too low, that the recoils lost more velocity in the target than was expected, and that more of them stopped in the target. These considerations were given weight in the assignment of a lifetime, but it was believed that they were not sure enough to dictate the values of $dv/d\rho$ to be used. It seems possible that the inclusion of the effects of large-angle scattering of the moving atoms for velocities less than

$(1.0)10^8$ centimeters per second might also tend to improve the shape of the calculated curve by lowering it for target positions in the region of 0.08 cm without much affecting the outer end.

Discussion of the Experimental Results

If one computes rough single particle limits for the 0.096-Mev transition in O^{19}, using the formulae given by Blatt and Weisskopf (26) with a radius of $(1.5)\ A^{1/3}\ 10^{-13}$ cm and without any additional statistical factors, one obtains the following estimates:

Multipolarity	Mean Life
E1	$(1.0)\ 10^{-12}$ seconds
M1	$(3.5)\ 10^{-11}$
E2	$(1.3)\ 10^{-5}$

The measured lifetime thus could be either a slow E1 or M1 transition (27). It is extremely unlikely that it is an E2 transition. A dipole transition between the 0.096-Mev state and a $J = 5/2$ ground state allows $J = 3/2$, $5/2$, or $7/2$ for the former state. However, only the possibilities $J^\pi = 3/2^\pm$, or $5/2^+$ are in agreement with those suggested in Part III B.

In regard to the possibility that the 1.47-Mev state might have a mean life of the order of the one observed it is again useful to take recourse to single particle estimates. The single particle estimate for the mean life of an E2

transition from the 1.47-Mev state to the ground state is $(1.6)10^{-11}$ seconds. If it be assumed that the 1.37-Mev transition is at least roughly a power of ten faster than the 1.47-Mev transition, then for the 1.37-Mev transition to have a mean life of the order of 10^{-9} seconds the speed of the 1.47-Mev transition would have to be more than 100 times slower than the single particle estimate. It may be noted that among the eight E2 transitions in light nuclei listed by Wilkinson (27) only one has a speed relative to its single particle estimate of this order and that this one is not too well established. It is true, however, as Wilkinson points out, that fast transitions are more likely to have been observed than the slow ones. Nevertheless, there appears to be some basis for believing that it is unlikely that the 1.47-Mev state would show a lifetime that would affect this measurement of the lifetime of the 0.096-Mev state.

One of the outstanding questions posed by the theoretical work of Elliott and Flowers (2) in regard to O^{19} is whether or not the 0.096-Mev state is indeed the $J^{\pi} = 3/2^{+}$ state that is predicted at roughly 0.5 Mev. Let it be assumed for the moment that the 1.47-Mev state accounts for the $J^{\pi} = 1/2^{+}$ state that is predicted for about the same excitation energy, 0.5 Mev. It is seen that $J^{\pi} = 3/2^{+}$ is one of the possibilities permitted by the experiments described above. It would be interesting to compute from the theoretical wave functions the M1 γ-ray transition rate between the $3/2^{+}$ state and the $5/2^{+}$ ground state and to compare the resulting lifetime with

the experimental one measured here.

It would also be interesting to determine whether the theoretical wave function for the $3/2^+$ state leads to a small neutron reduced width for this state and thus accounts for the lack of stripping in its formation. That this is likely to be the case may be seen by an examination of the jj-coupling decompositions of the theoretical wave functions for the O^{18} ground state and for the O^{19} $3/2^+$ state. The $J = 0^+$ ground state of O^{18} is described as having a configuration for two neutrons outside of an unexcited O^{16} core which is 79 percent $(d_{5/2})^2$, 6 percent $(d_{3/2})^2$, and 15 percent $(s_{1/2})^2$. In order to form a $3/2^+$ state of O^{19} by stripping, a $d_{3/2}$ neutron must be added to this configuration. However, the predicted configuration of the three neutrons outside of the O^{16} core for the $3/2^+$ state in O^{19} is 62 percent $(d_{5/2})^3$, 33 percent $(d_{5/2})^2(s_{1/2})$, 2 percent $(d_{5/2})(d_{3/2})(s_{1/2})$, and 3 percent $(d_{5/2})^2(d_{3/2})$. Only the last of these four terms is seen to be of the right form for stripping formation.

An interesting extension of the experimental work would be to determine the internal conversion coefficient of the 0.096-Mev γ-ray transition. The K-shell conversion coefficient for an E1 transition is estimated to be $(1.9)10^{-3}$ while that for an M1 transition is estimated to be $(5.9)10^{-4}$ (Reference 28). Thus one could hope to determine the multipolarity of the radiation and the parity of the 0.096-Mev state.

IV REFERENCES

(1) J. P. Elliott and B. H. Flowers, Proc. Roy. Soc. Lond. 242A, 57 (1957).

(2) J. P. Elliott and B. H. Flowers, Proc. Roy. Soc. Lond. 229A, 536 (1955).

(3) M. G. Redlich, Phys. Rev. 98, 199 (1955); Phys. Rev. 99, 1427 (1955).

(4) F. Ajzenberg and T. Lauritsen, Energy Levels of Light Nuclei, V, Revs. Modern Phys. 27, 77 (1955).

(5) B. J. Toppel, Phys. Rev. 103, 141 (1956).

(6) A portion of the work presented in Part II A has been described by the author in the following reference: W. Zimmermann, Jr., Phys. Rev. 104, 387 (1956).

(7) S. T. Butler, Nuclear Stripping Reactions, Horwitz, Sydney (1957). This reference and the following one are valuable sources of information concerning work that has been published about stripping reactions.

(8) R. Huby, Stripping Reactions, Chapter 7 in Progress in Nuclear Physics, Vol. 3, edited by O. R. Frisch, Academic Press, New York (1953).

(9) W. Whaling, The Energy Loss of Charged Particles in Matter, Page 193 in Handbuch der Physik, Vol. 34, edited by S. Flügge, Springer (1958).

(10) C. R. Lubitz, Numerical Table of Butler-Born Approximation Stripping Cross Sections, University of Michigan (1957). Formula (10) in this paper is essentially the simple Butler formula given as formula (3-26) in

reference (7) if one takes the reduced width, γ_{l_c}, to be $\frac{\hbar^2}{2m_{ni}} r_o R_{nl}(r_o)^2$ in the notation of Lubitz. It then follows that

$$\theta^2 = \frac{r_o^3}{3} R_{nl}(r_o)^2.$$

(11) E. K. Warburton and J. N. McGruer, Phys. Rev. 105, 639 (1957).

(12) D. H. Wilkinson, Phys. Rev. 105, 686 (1957).

(13) J. M. Freeman and R. C. Hanna, Nuclear Physics 4, 599 (1957).

(14) Toppel, Wilkinson, and Alburger, Phys. Rev. 101, 1485 (1956).

(15) Stratton, Blair, Famularo, and Stuart, Phys. Rev. 98, 629 (1955).

(16) S. Bashkin and G. Goldhaber, Rev. Sci. Inst. 22, 112 (1951).

(17) Holmgren, Blair, Famularo, Stratton, and Stuart, Rev. Sci. Inst. 25, 1026 (1954).

(18) K. Ahnlund, Arkiv för Physik 10, 425 (1956).

(19) R. V. Popić, Nuovo Cimento IV, 1597 (1956).

(20) Devons, Manning, and Towle, Proc. Phys. Soc. Lond. 69A, 173 (1956).

(21) Evans, Stier, and Barnett, Phys. Rev. 90, 825 (1953).

(22) P. M. S. Blackett and D. S. Lees, Proc. Roy Soc. Lond. 134, 658 (1932).

(23) K. O. Nielson, The Range of Atomic Particles with Energies about 50 kev, Chapter 9 in Electromagnetically Enriched Isotopes and Mass Spectrometry, edited by

M. L. Smith, Academic Press, New York (1956).

(24) Bonner, Eisinger, Kraus, and Marion, Phys. Rev. 101, 209 (1956).

(25) McEllistrem, Jones, Chiba, Douglas, Herring, and Silverstein, Phys. Rev. 104, 1008 (1956).

(26) J. M. Blatt and V. F. Weisskopf, Theoretical Nuclear Physics, Wiley, New York (1952), page 627.

(27) D. H. Wilkinson, Phil. Mag. 1, 127 (1956).

(28) W. R. Mills, Jr., Thesis, California Institute of Technology (1955).

Table I: Proton Angular Distributions for the $N^{15}(d,p)N^{16}$ Reaction at a Deuteron Energy of 2.75 Mev

	Final State of N^{16}				
	0 Mev	0 Mev	0.119 Mev	0.293 Mev	0.392 Mev
Proton Angle			Relative Yields		
θ_{cm}	Uncorrected	Corrected			
7.6°	860		3220	360	13870
10.9°	780±50	-30±80	2880±200	400	11480±700
16.4°	770	180	2140	500	9520
21.8°	780	330	1500	730	6810
27.2°	810	530	810	890	4090
32.6°	850±60	680±60	380±30	1130±80	2320±160
38.0°	900		190	1300	1100
43.3°	960	920	180	1460	580
48.7°	890		250	1410	540
54.0	940	930	400	1520	680
59.3°	940		550	1470	960
64.5°	910	890	680	1340	1230
69.7°	800		684	1190	1520
74.8°	760±50	710	710±50	1020±70	1600±100
80.0°	720		700	840	1700
85.1°	660	600	640	780	1790
90.2°	540		560	580	1650
95.2°	540	470	470	540	1580
100.1°	460		370	390	1400
105.1°	470	410	310	350	1180
110.0°	490		310	310	1150
114.8°	480±30	420	250±20	310±20	1090±70
119.7°	460		220	280	880
124.5°	590	540	150	310	900
129.3°	660		120	300	760
134.0°	610±40	580	90±10	400±30	670±40
138.7°	700		70	400	600
143.3°	650	610	70	470	530

Table IV: Proton Angular Distributions for the $O^{18}(d,p)O^{19}$ Reaction at a Deuteron Energy of 1.74 Mev

	Final State of O^{19}			Final State of O^{19}
	0 Mev	0.096 Mev		1.47 Mev
Proton Angle θ_{cm}	Relative Yields		Proton Angle θ_{cm}	Relative Yield
			10.7°	5310
			16.0°	4700
21.0°	380±10	115±6	21.4°	3740±40
26.3°	410	125	26.7°	3000
31.5°	470	120	32.0°	2260
			37.3°	1730
41.9°	570	130	42.6°	1330
52.3°	590±15	130±7	53.1°	1000±20
62.6°	590	130	63.5°	1130
72.8°	530	120	73.8°	1440
83.0°	430	105	84.0°	1710
93.0°	330±10	85±6	94.0°	1750±25
103.0°	250	70	104.0°	1750
112.8°	230	55	113.8°	1670
122.6°	230	50	123.5°	1520
132.3°	240±10	50±5	133.1°	1370±25
141.9°	270	55	142.6°	1270

Table V: Proton Angular Distributions for the $O^{18}(d,p)O^{19}$ Reaction at a Deuteron Energy of 2.50 Mev

	Final State of O^{19}	
	0 Mev	0.096 Mev
Proton Angle θ_{cm}	Relative Yields	
10.6°	210±15	102±8
15.9°	280	99
21.1°	370	94
26.4°	490	98
31.7°	610	109
36.9°	750	103
42.1°	840	117
47.4°	920	102
52.6°	1010±40	111±7
57.7°	980	104
62.9°	890	94
68.0°	820	80
73.1°	710	90
78.2°	590	87
83.3°	530	92
88.3°	420	73
93.3°	390±15	80±5
98.3°	350	
103.3°	340	72
108.2°	320	
113.1°	280	87
118.0°		110
122.9°	290	119
127.7°		133
132.6°	320±30	121±13
137.4°	360	128
142.1°	360	

Table VI: Proton Excitation Curves for the $O^{18}(d,p)O^{19}$ Reaction at a Laboratory Angle of 90°

Ed Mev	Final State of O^{19} Relative Yields		
	0 Mev	0.096 Mev	1.47 Mev
1.695	350	65	1610
1.705	320±25	60±6	1670±110
1.715	360	75	1650
1.730	330	80	1660
1.740	340	85	1690
1.750	340	85	1720
1.765	360	90	1690
1.775	380	105	1780
1.785	380	105	1780
1.805	350	85	
1.820	380	85	
1.835	360	95	
1.850	360	110	
1.860	410	120	
1.875	430	125	
1.890	410	125	
1.905	430	115	
1.915	450	105	
1.930	440	105	
1.945	470	100	
1.955	470	110	
1.970	480	115	
1.985	510	150	
2.000	510±35	110±10	
2.010	560	75	
2.025	550	75	
2.040	540	75	
2.055	530	70	
2.065	510	70	
2.080	510	75	
2.095	460	65	
2.105	450	90	
2.120	440	100	
2.135	440	90	
2.150	400	85	
2.160	420	105	
2.175	420	110	
2.190	410	105	

Ed Mev	Final State of O^{19} Relative Yields	
	0 Mev	0.096 Mev
2.205	440	105
2.215	410	90
2.230	410	85
2.245	420	90
2.255	420	80
2.270	380	85
2.285	380	85
2.300	370±25	80±8
2.310	420	85
2.325	440	70
2.340	430	80
2.355	430	75
2.365	420	75
2.380	420	80
2.395	410	80
2.405	460	85
2.420	430	90
2.435	420	85
2.450	390	95
2.460	470	90
2.475	410	75
2.490	450	80
2.505	430	80
2.515	430	85
2.530	410	90
2.545	380	
2.555	390	
2.570	360	
2.585	370	
2.600	370±25	
2.610	390	
2.625	340	
2.640	350	
2.655	370	
2.665	390	
2.680	360	
2.695	360	
2.710	330	
2.720	350	

Table VII: Proton Angular Distribution for the $O^{16}(d,p)O^{17}$ Reaction at a Deuteron Energy of 2.50 Mev

	Final State of O^{17}
	0 Mev
Proton Angle θ cm	Relative Yield
10.6°	6030±370
15.9°	6000
21.2°	5970
26.5°	6140
31.8°	6920
37.1°	7010
42.3°	7410
47.6°	7430
52.8°	7310±260
58.0°	6950
63.2°	6400
68.3°	5840
73.4°	5240
78.5°	4290
83.6°	4280
88.6°	3730
93.6°	3990±80
98.6°	
103.6°	4390
108.5°	
113.4°	4960
118.3°	
123.2°	6080
128.0°	6220
132.8°	7030±350
137.6°	7450
142.3°	7680

Table VIII: Proton Excitation Curve for the $O^{16}(d,p)O^{17}$ Reaction at a Laboratory Angle of 90°

Final State of O^{17} 0 Mev		Final State of O^{17} 0 Mev	
Ed Mev	Relative Yield	Ed Mev	Relative Yield
1.805	2240	2.340	4930
1.820	2220	2.355	4380
1.835	2290	2.365	3950
1.850	2510	2.380	3670
1.860	2850	2.395	3290
1.875	3570	2.405	2890
1.890	3820	2.420	2970
1.905	3310	2.435	3090
1.915	2510	2.450	3500
1.930	2270	2.460	4060
1.945	2090	2.475	3650
1.955	1940	2.490	3860
1.970	1930	2.505	3980
1.985	1920	2.515	3860
2.000	1990±130	2.530	4160
2.010	1870	2.545	5020
2.025	1870	2.555	3710
2.040	1910	2.570	3340
2.055	1970	2.585	3310
2.065	1980	2.600	3570±230
2.080	2110	2.610	3690
2.095	2180	2.625	3890
2.105	2180	2.640	4130
2.120	2330	2.655	4350
2.135	2380	2.665	4560
2.150	2330	2.680	5010
2.160	2290	2.695	5070
2.175	2360	2.710	5480
2.190	2390	2.720	5600
2.205	2290		
2.215	2450		
2.230	3240		
2.245	3890		
2.255	4370		
2.270	4680		
2.285	5340		
2.300	5630±360		
2.310	5740		
2.325	5410		

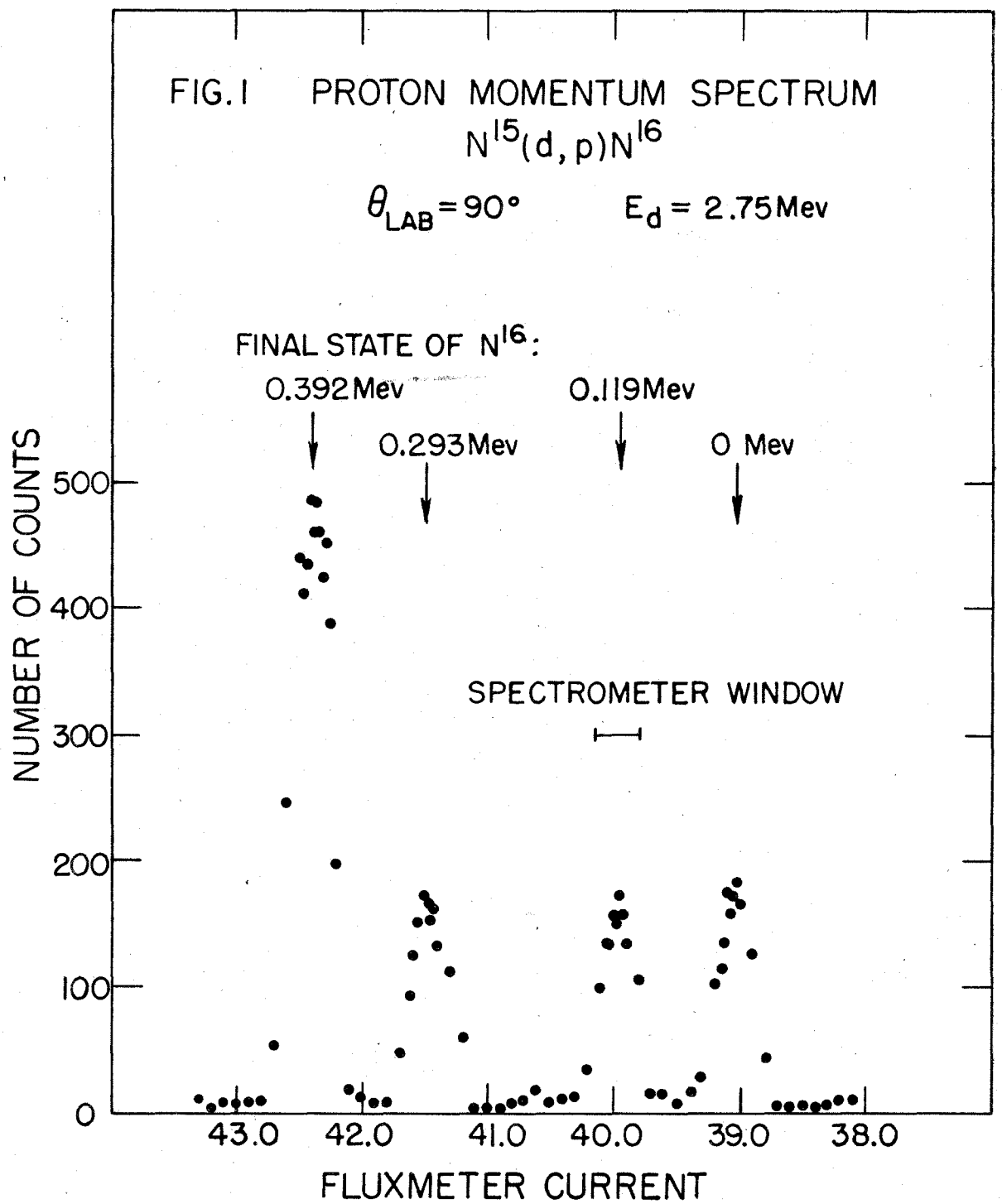
FIG. 1 PROTON MOMENTUM SPECTRUM
$N^{15}(d,p)N^{16}$
$\theta_{LAB} = 90°$ $E_d = 2.75$ Mev
FINAL STATE OF N^{16}:
0.392 Mev
0.293 Mev
0.119 Mev
0 Mev
SPECTROMETER WINDOW
NUMBER OF COUNTS
0
100
200
300
400
500
43.0
42.0
41.0
40.0
39.0
38.0
FLUXMETER CURRENT

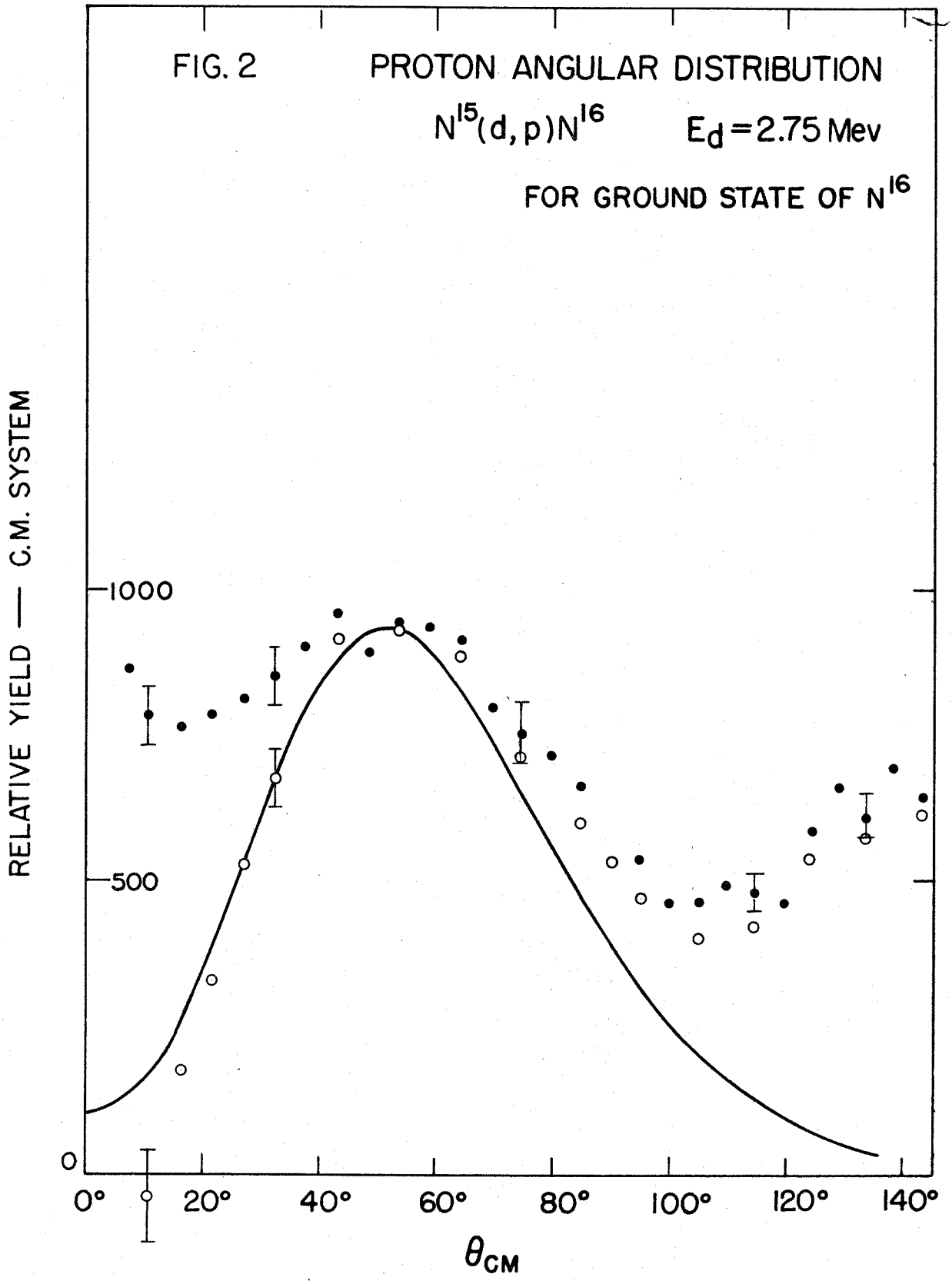
FIG. 2
PROTON ANGULAR DISTRIBUTION
$N^{15}(d,p)N^{16}$ $E_d = 2.75$ Mev
FOR GROUND STATE OF N^{16}
RELATIVE YIELD — C.M. SYSTEM
1000
500
0
0°
20°
40°
60°
80°
100°
120°
140°
θ_{CM}

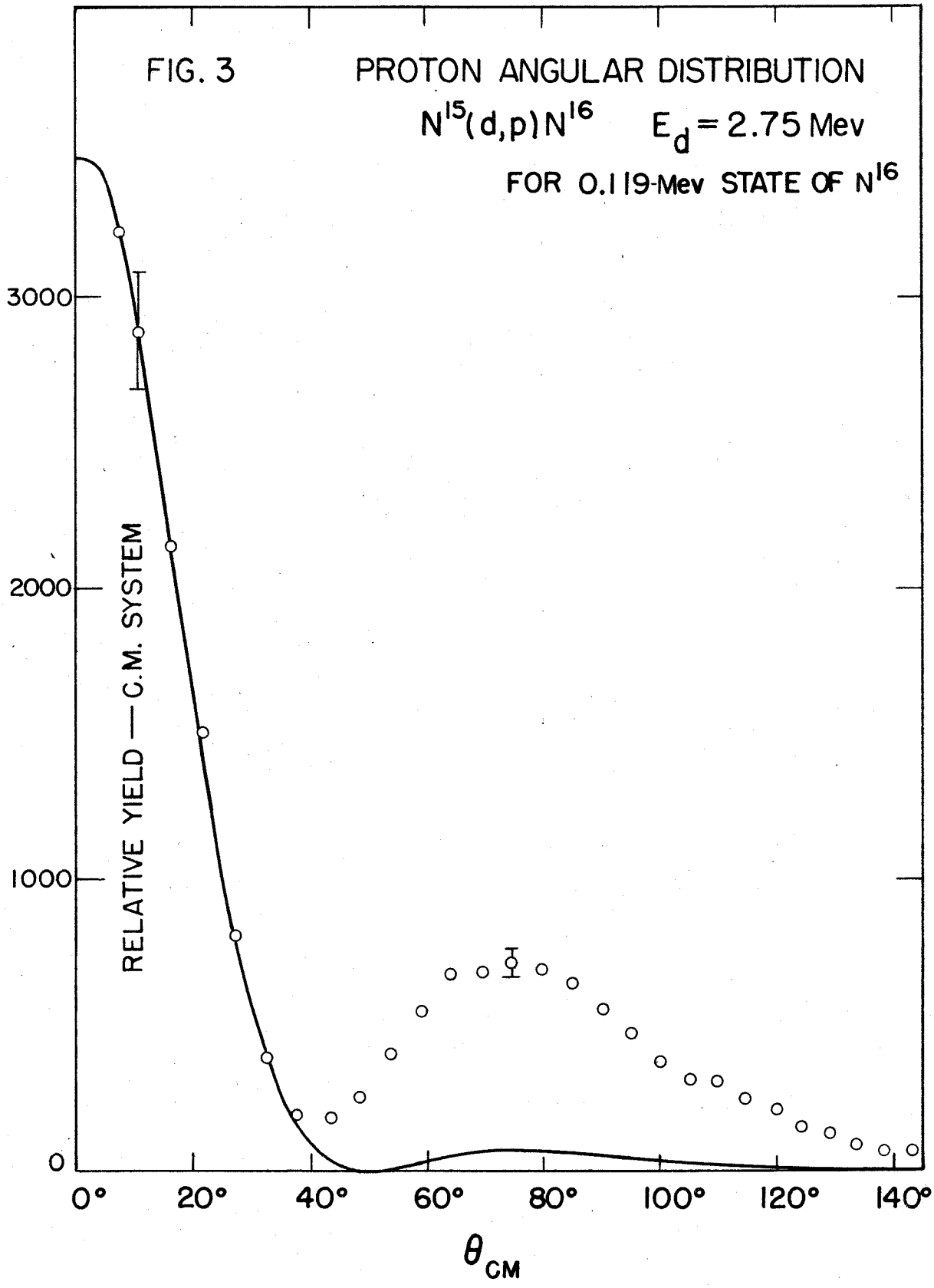
FIG. 3
PROTON ANGULAR DISTRIBUTION
$N^{15}(d,p)N^{16}$ $E_d = 2.75$ Mev
FOR 0.119-Mev STATE OF N^{16}
RELATIVE YIELD — C.M. SYSTEM
3000
2000
1000
0
0°
20°
40°
60°
80°
100°
120°
140°
θ_{CM}

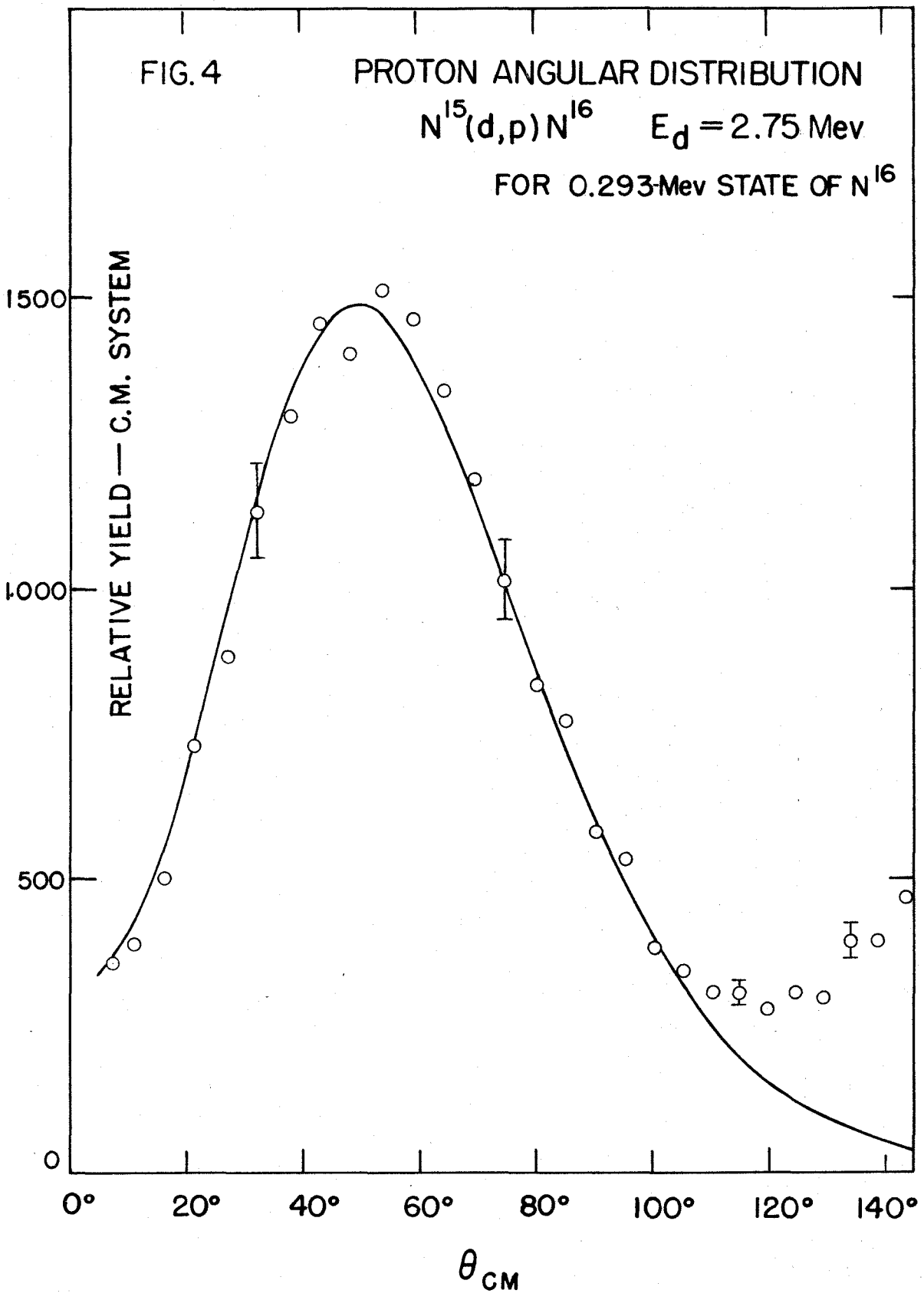
FIG. 4
PROTON ANGULAR DISTRIBUTION
$N^{15}(d,p)N^{16}$ $E_d = 2.75$ Mev
FOR 0.293-Mev STATE OF N^{16}
RELATIVE YIELD — C.M. SYSTEM
1500
1000
500
0
0°
20°
40°
60°
80°
100°
120°
140°
θ_{CM}

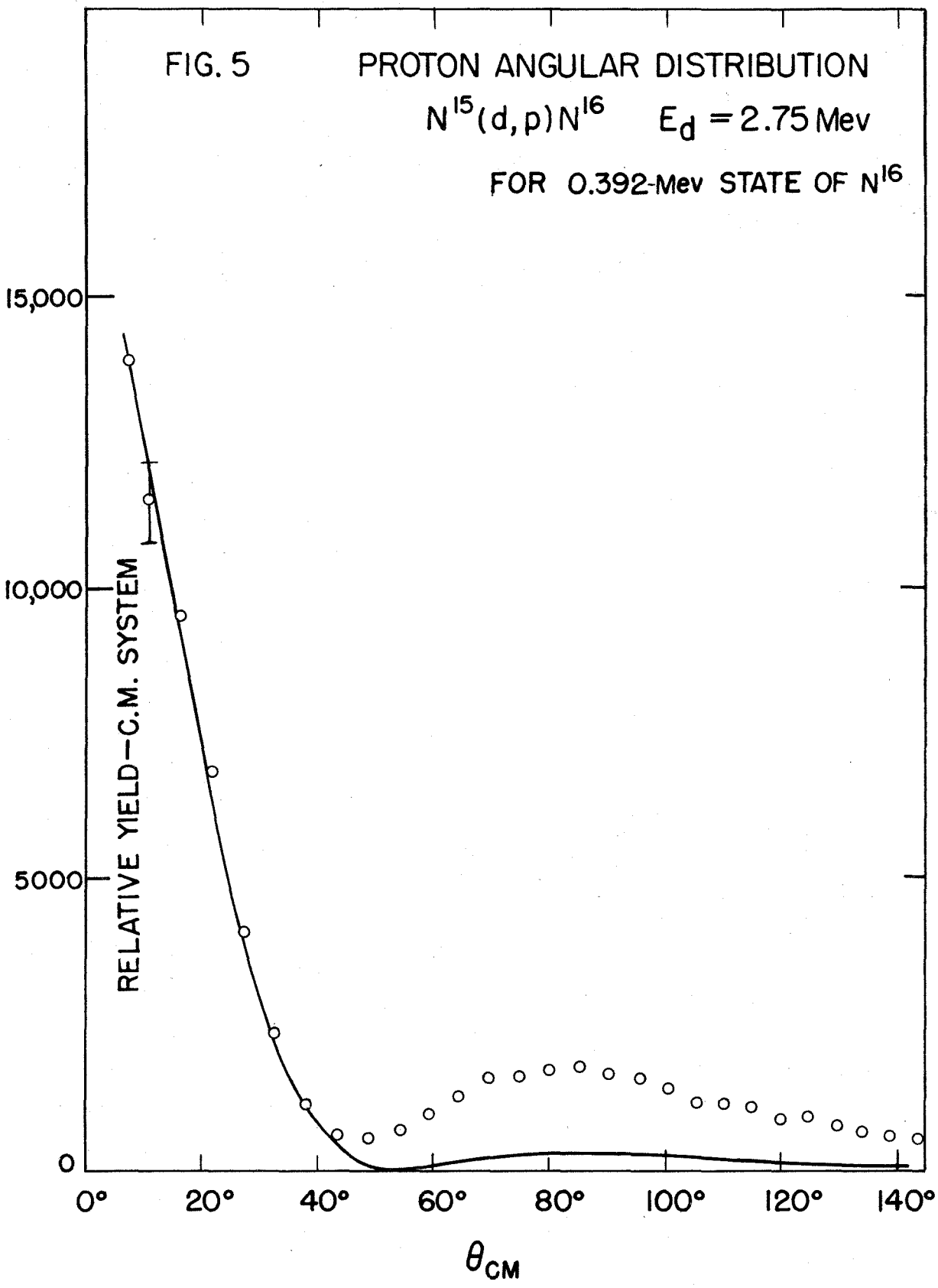
FIG. 5
PROTON ANGULAR DISTRIBUTION
$N^{15}(d,p)N^{16}$ $E_d = 2.75$ Mev
FOR 0.392-Mev STATE OF N^{16}
15,000
10,000
5000
0
RELATIVE YIELD—C.M. SYSTEM
0°
20°
40°
60°
80°
100°
120°
140°
θ_{CM}

FIG. 7 LIFETIME OF 0.119-Mev STATE OF N^{16}

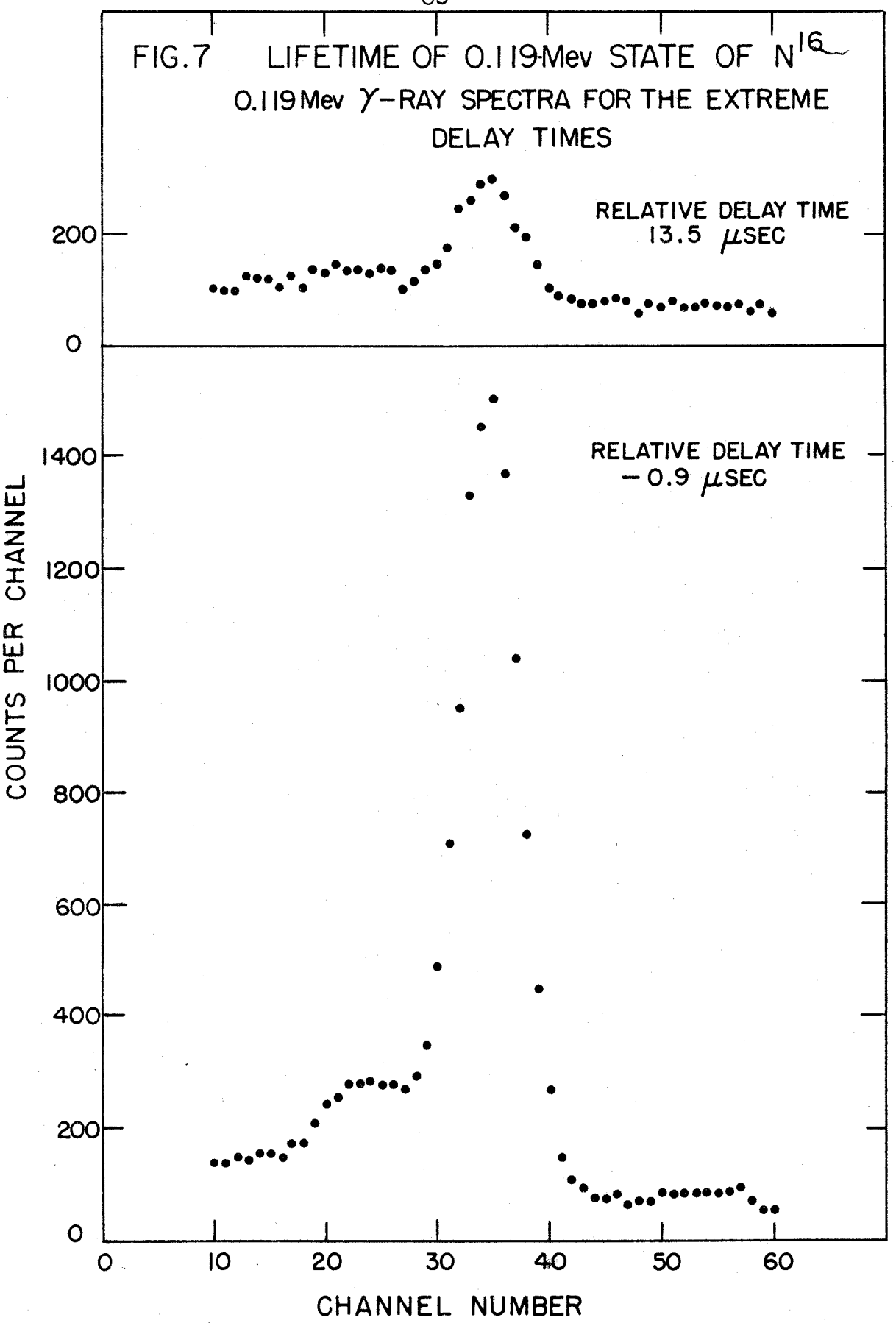

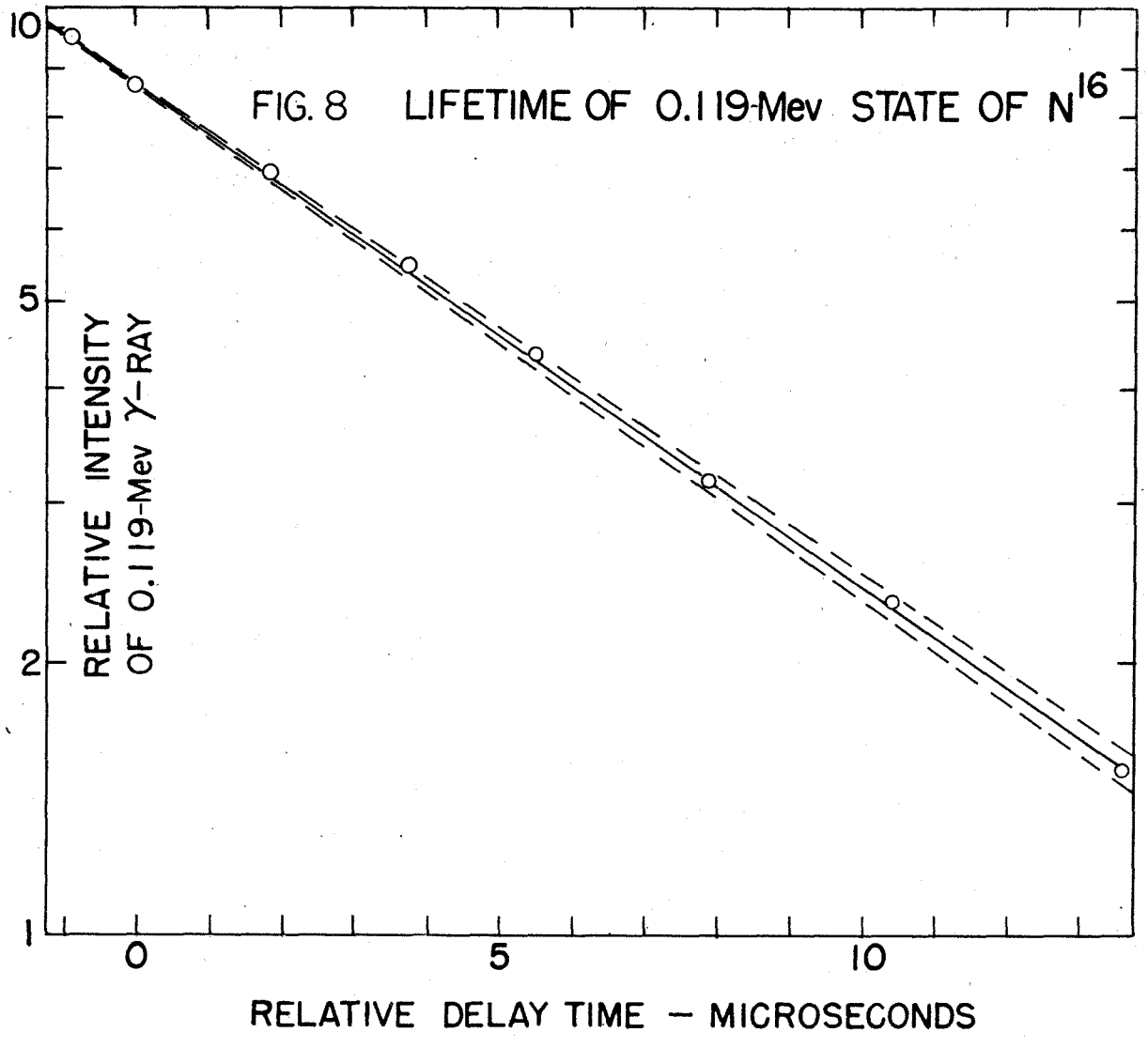
FIG. 8 LIFETIME OF 0.119-Mev STATE OF N^{16}
RELATIVE INTENSITY OF 0.119-Mev γ-RAY
10
5
2
1
0
5
10
RELATIVE DELAY TIME — MICROSECONDS

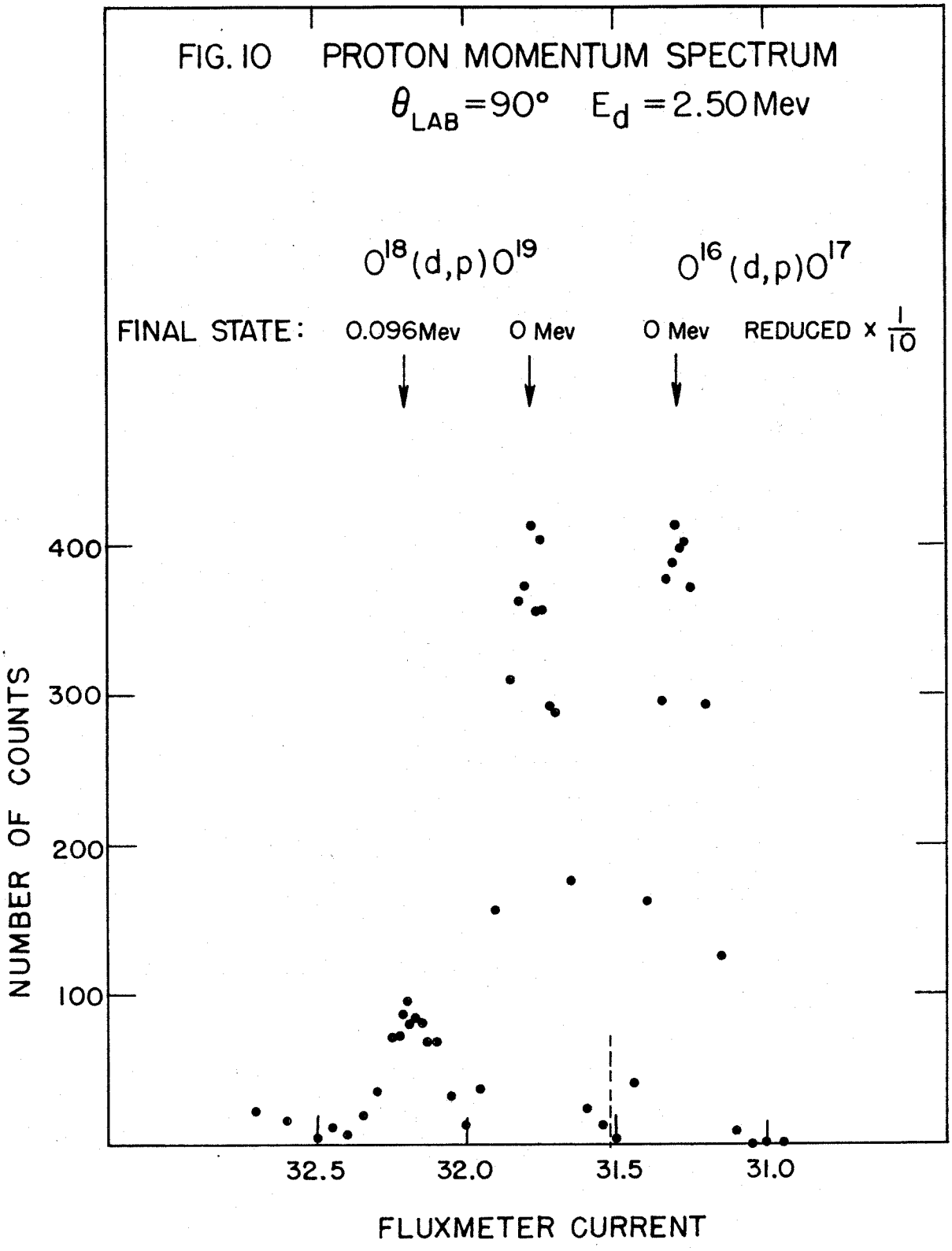
FIG. 10 PROTON MOMENTUM SPECTRUM
$\theta_{LAB} = 90°$ $E_d = 2.50$ Mev
$O^{18}(d,p)O^{19}$
$O^{16}(d,p)O^{17}$
FINAL STATE: 0.096Mev 0 Mev 0 Mev REDUCED x 1/10
NUMBER OF COUNTS
400
300
200
100
32.5
32.0
31.5
31.0
FLUXMETER CURRENT

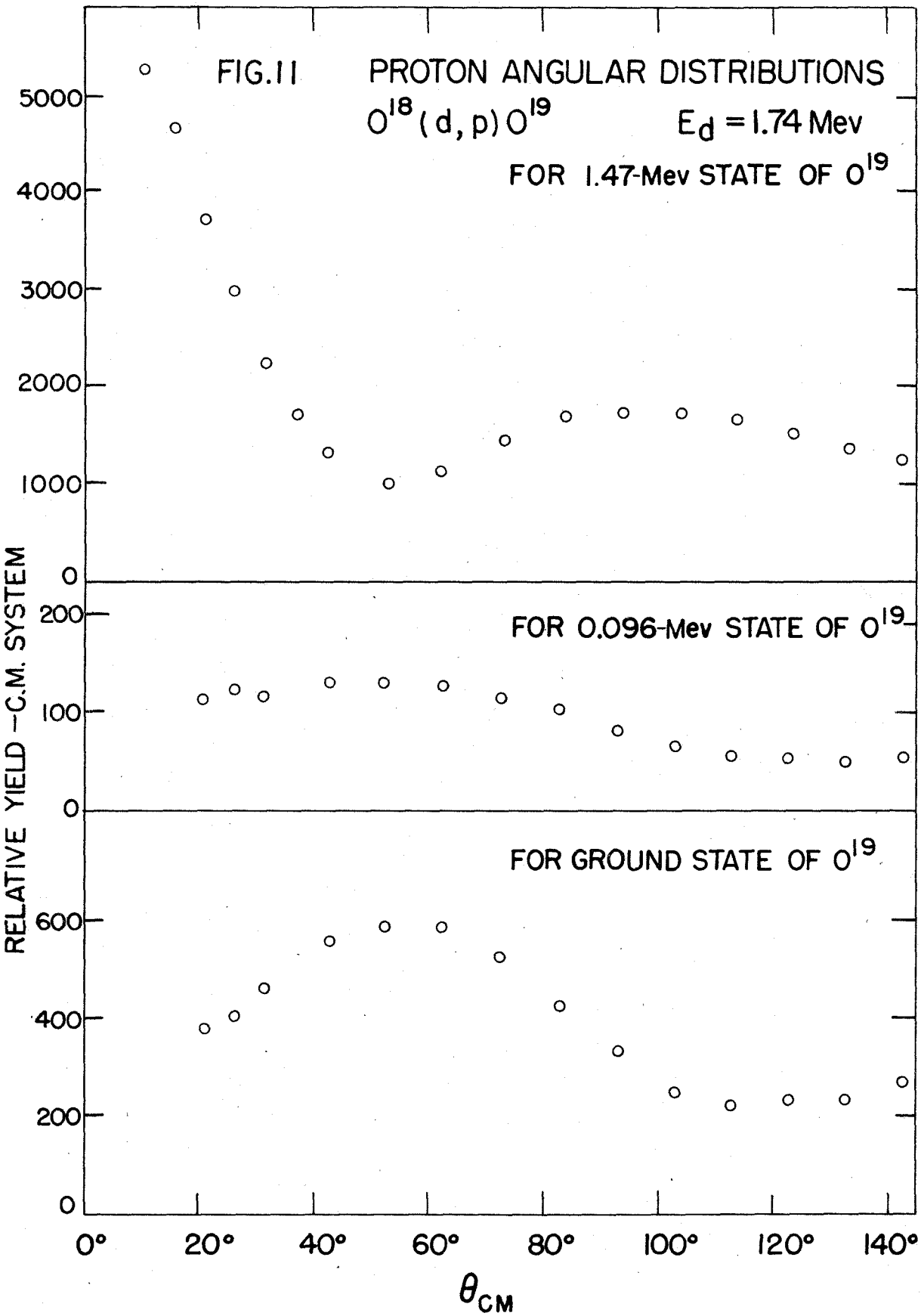
FIG.11 PROTON ANGULAR DISTRIBUTIONS
$O^{18}(d,p)O^{19}$ $E_d = 1.74$ Mev
FOR 1.47-Mev STATE OF O^{19}
FOR 0.096-Mev STATE OF O^{19}
FOR GROUND STATE OF O^{19}
RELATIVE YIELD —C.M. SYSTEM
5000
4000
3000
2000
1000
0
200
100
0
600
400
200
0
0°
20°
40°
60°
80°
100°
120°
140°
θ_{CM}

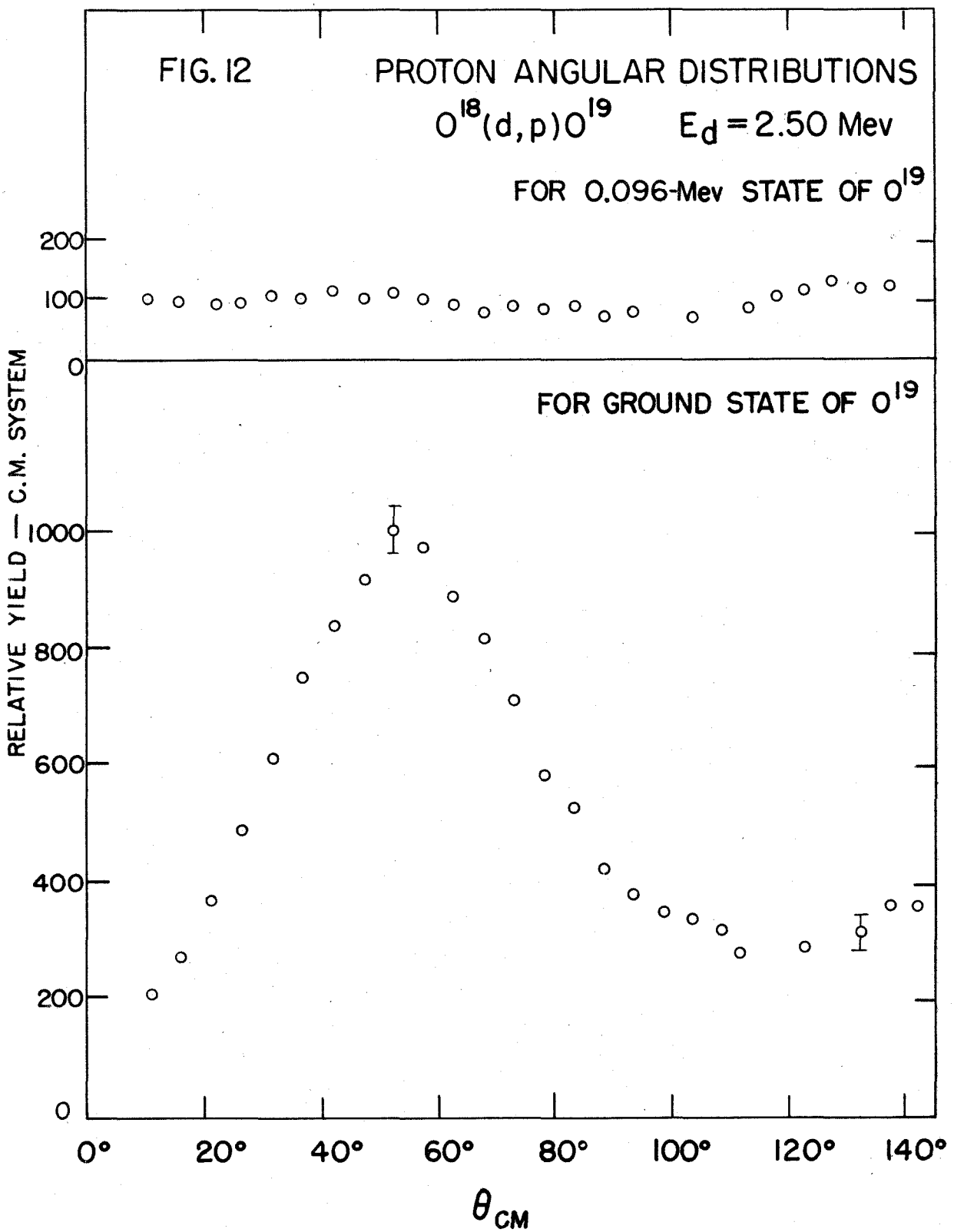
FIG. 12
PROTON ANGULAR DISTRIBUTIONS
$O^{18}(d,p)O^{19}$ $E_d = 2.50$ Mev
FOR 0.096-Mev STATE OF O^{19}
FOR GROUND STATE OF O^{19}
RELATIVE YIELD — C.M. SYSTEM
200
100
0
1000
800
600
400
200
0
0°
20°
40°
60°
80°
100°
120°
140°
θ_{CM}

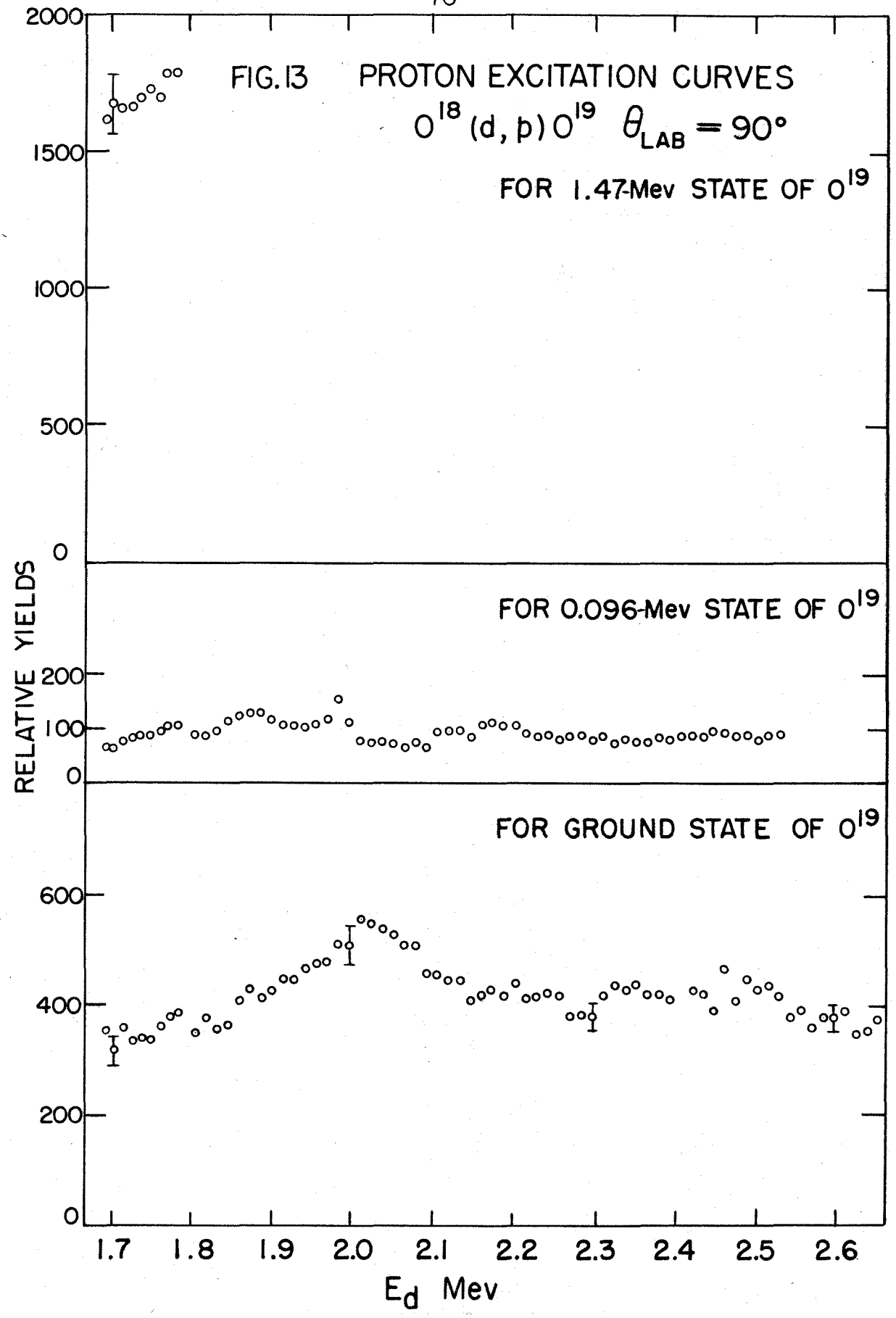
FIG. 13 PROTON EXCITATION CURVES
$O^{18}(d,p)O^{19}$ $\theta_{LAB} = 90°$
FOR 1.47-Mev STATE OF O^{19}
FOR 0.096-Mev STATE OF O^{19}
FOR GROUND STATE OF O^{19}
RELATIVE YIELDS
2000
1500
1000
500
0
200
100
0
600
400
200
0
1.7
1.8
1.9
2.0
2.1
2.2
2.3
2.4
2.5
2.6
E_d Mev

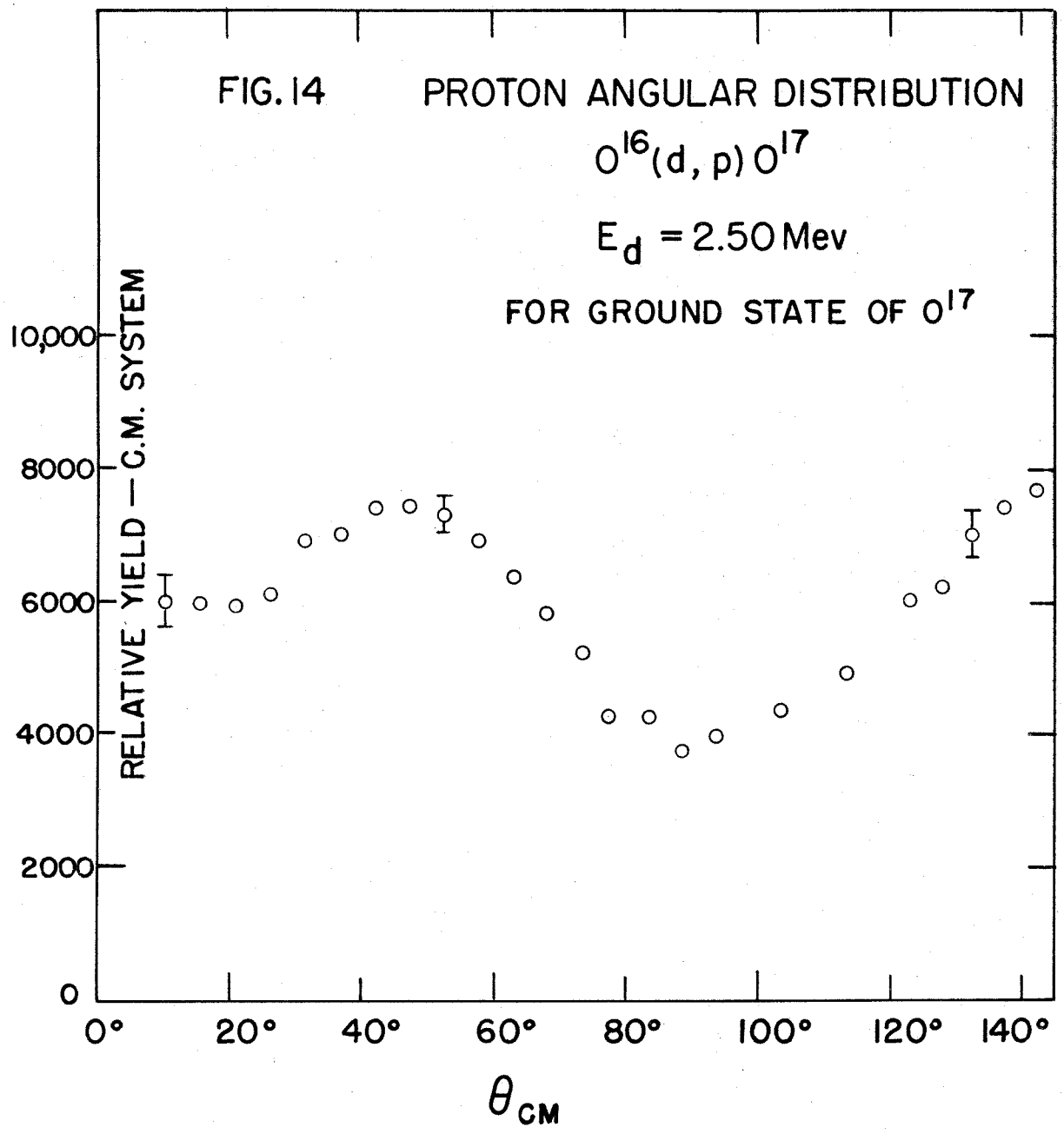
FIG. 14
PROTON ANGULAR DISTRIBUTION
$O^{16}(d, p) O^{17}$
$E_d = 2.50$ Mev
FOR GROUND STATE OF O^{17}
RELATIVE YIELD — C.M. SYSTEM
10,000
8000
6000
4000
2000
0
0°
20°
40°
60°
80°
100°
120°
140°
θ_{CM}

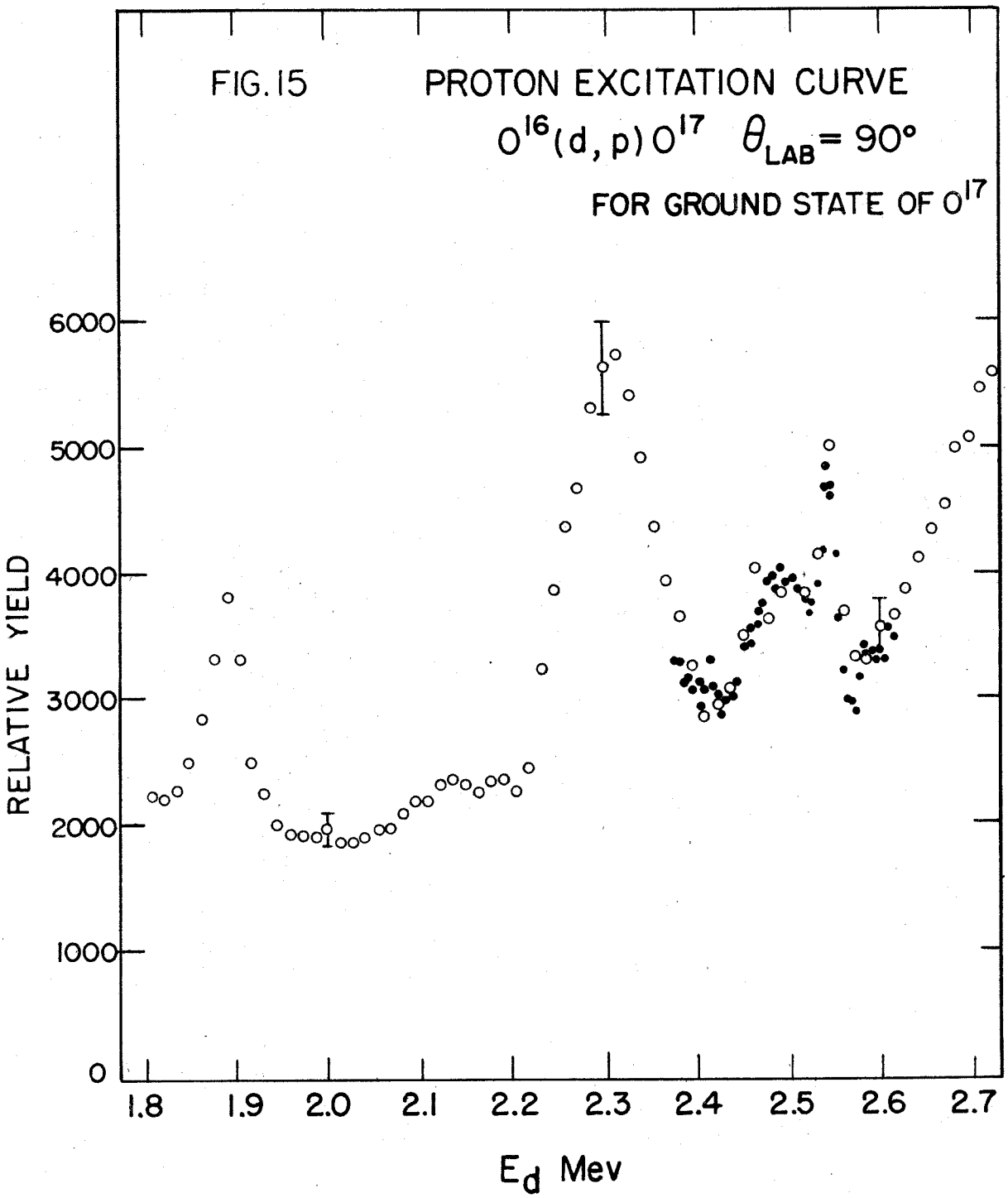
FIG. 15
PROTON EXCITATION CURVE
$O^{16}(d,p)O^{17}$ $\theta_{LAB} = 90°$
FOR GROUND STATE OF O^{17}
RELATIVE YIELD
6000
5000
4000
3000
2000
1000
0
1.8
1.9
2.0
2.1
2.2
2.3
2.4
2.5
2.6
2.7
E_d Mev

FIG. 16 DETAIL OF RECOIL APPARATUS

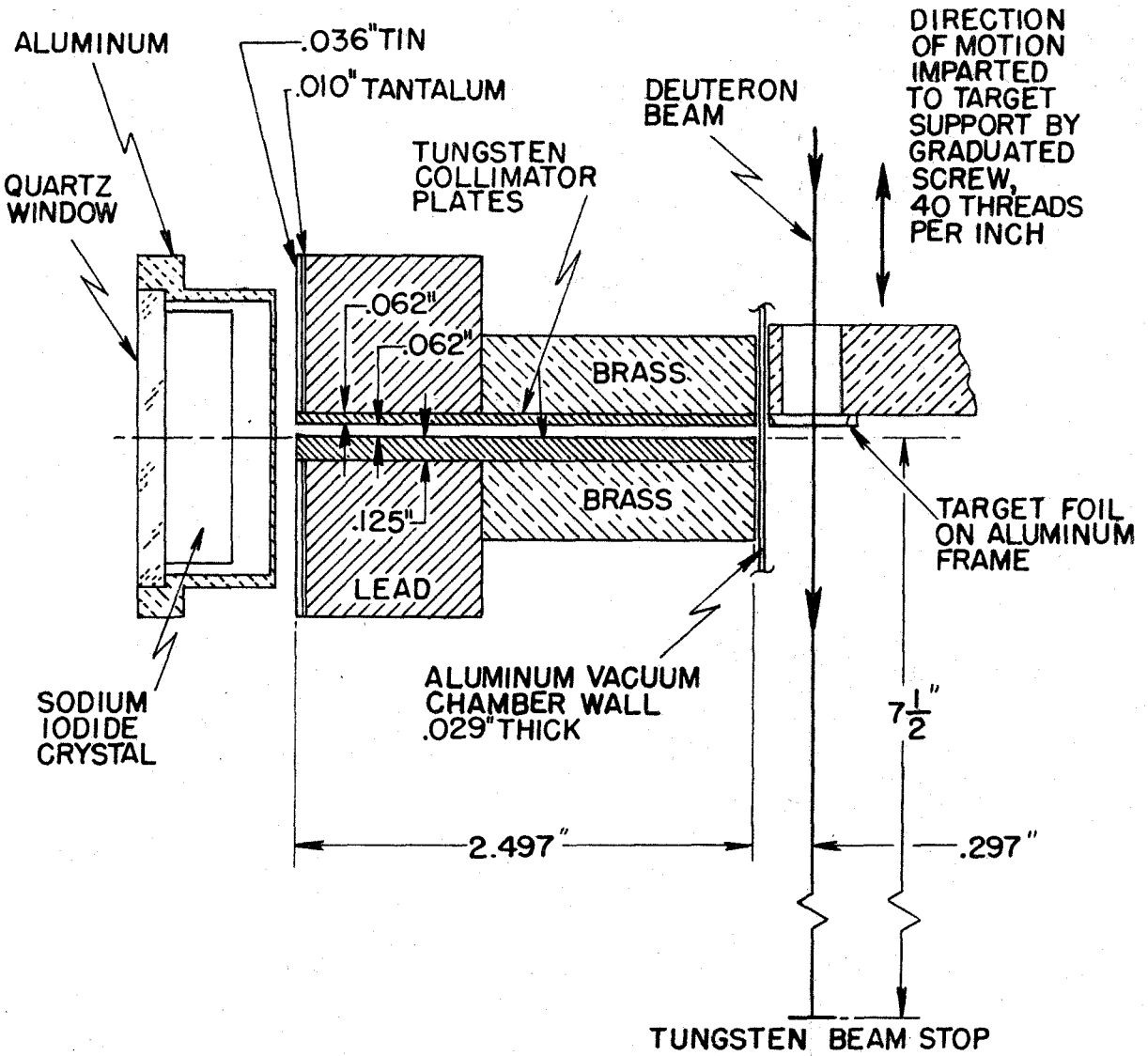

FIG. 17 RECOIL γ-RAY SPECTRA FOR VARIOUS TARGET POSITIONS

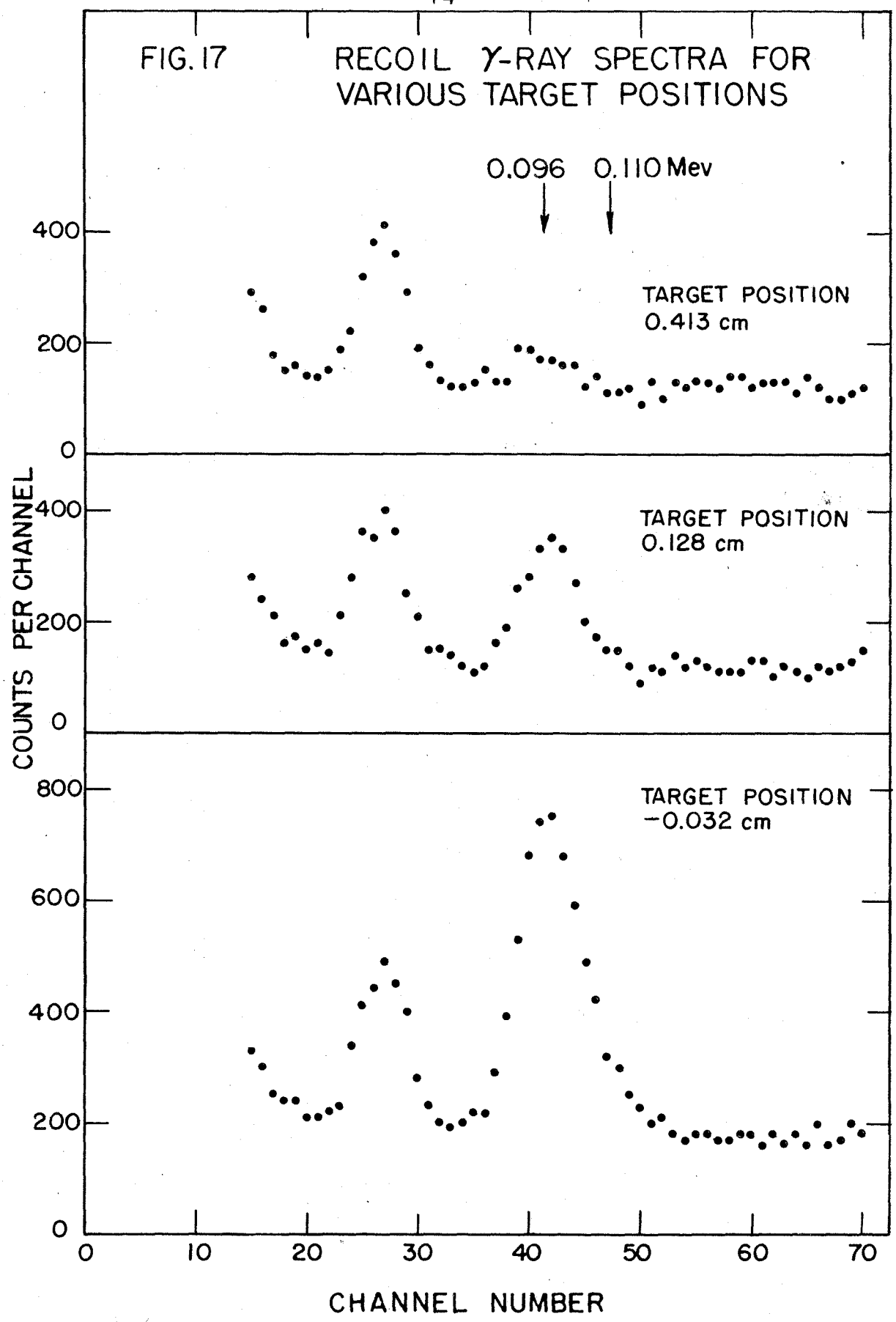

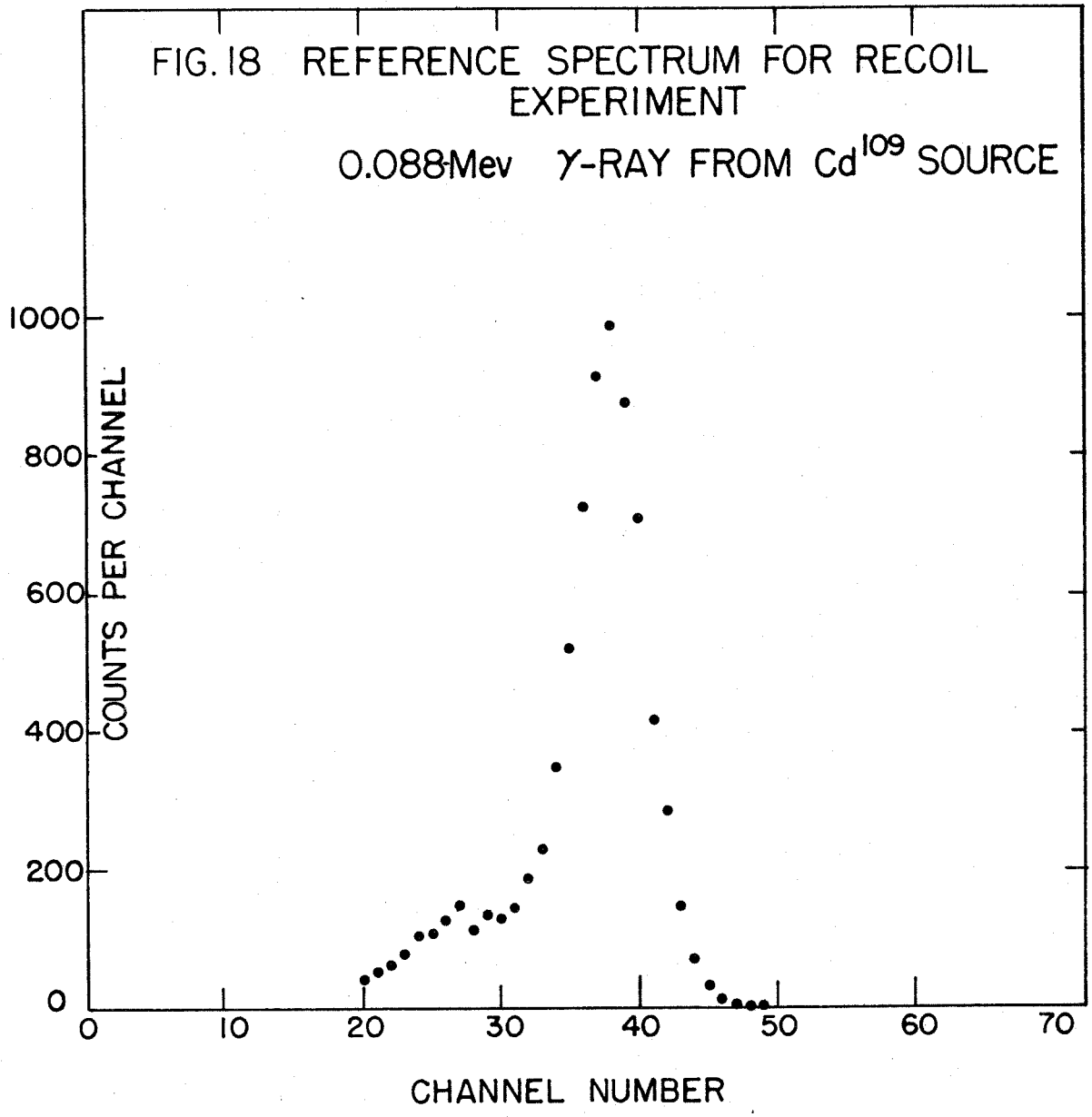
FIG. 18 REFERENCE SPECTRUM FOR RECOIL EXPERIMENT
0.088-Mev γ-RAY FROM Cd109 SOURCE
COUNTS PER CHANNEL
1000
800
600
400
200
0
0
10
20
30
40
50
60
70
CHANNEL NUMBER

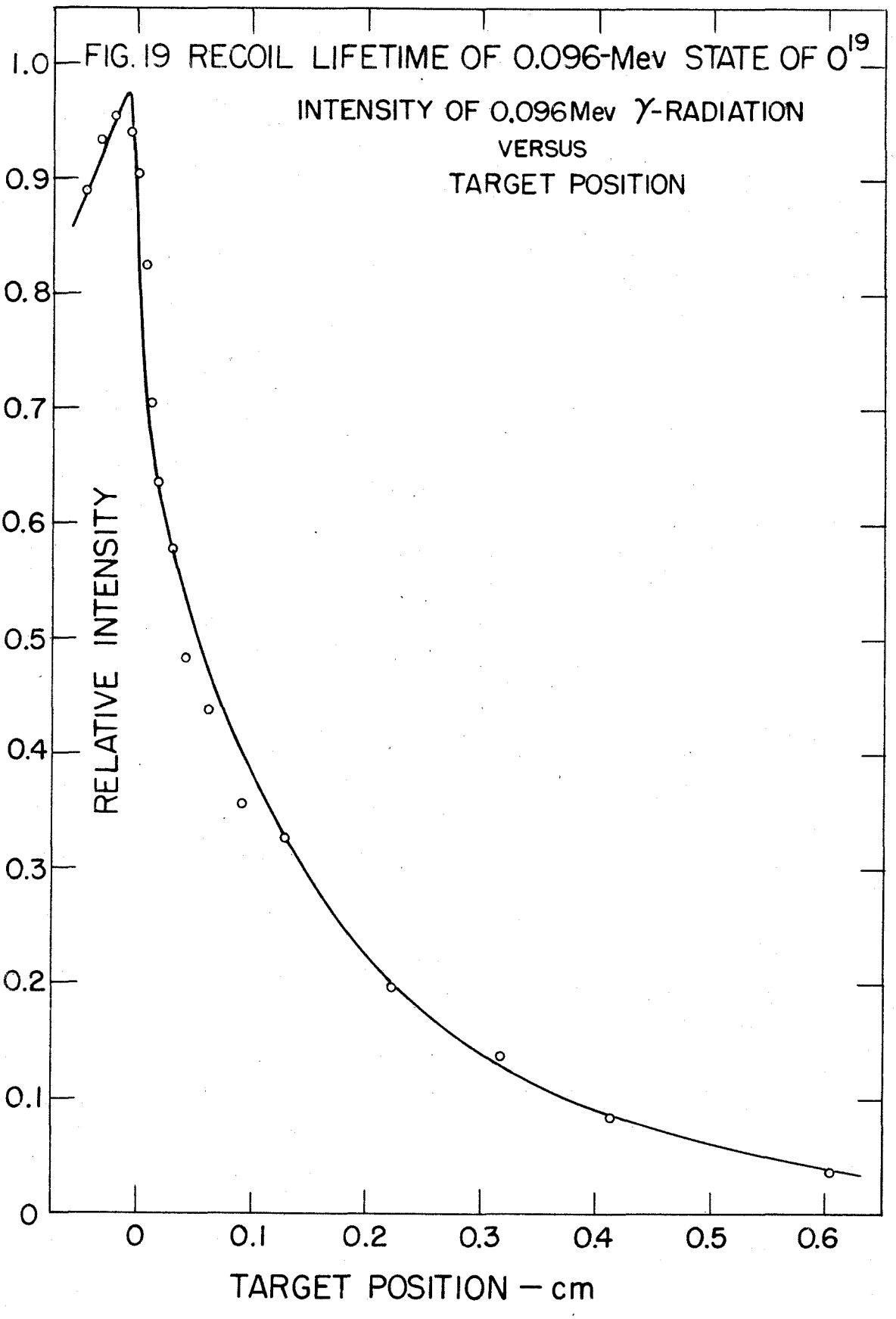
FIG. 19 RECOIL LIFETIME OF 0.096-Mev STATE OF O19
INTENSITY OF 0.096 Mev γ-RADIATION
VERSUS
TARGET POSITION
RELATIVE INTENSITY
1.0
0.9
0.8
0.7
0.6
0.5
0.4
0.3
0.2
0.1
0
0
0.1
0.2
0.3
0.4
0.5
0.6
TARGET POSITION — cm